



**HAL**  
open science

## Performance Study of Two Serial Interconnected Chemostats with Mortality

Manel Dali-Youcef, Alain Rapaport, Tewfik Sari

► **To cite this version:**

Manel Dali-Youcef, Alain Rapaport, Tewfik Sari. Performance Study of Two Serial Interconnected Chemostats with Mortality. *Bulletin of Mathematical Biology*, 2022, 84 (10), 10.1007/s11538-022-01068-6 . hal-03762535

**HAL Id: hal-03762535**

**<https://hal.inrae.fr/hal-03762535>**

Submitted on 28 Aug 2022

**HAL** is a multi-disciplinary open access archive for the deposit and dissemination of scientific research documents, whether they are published or not. The documents may come from teaching and research institutions in France or abroad, or from public or private research centers.

L'archive ouverte pluridisciplinaire **HAL**, est destinée au dépôt et à la diffusion de documents scientifiques de niveau recherche, publiés ou non, émanant des établissements d'enseignement et de recherche français ou étrangers, des laboratoires publics ou privés.



Distributed under a Creative Commons Attribution 4.0 International License

# Performance study of two serial interconnected chemostats with mortality

Manel Dali-Youcef<sup>1,3</sup>, Alain Rapaport<sup>1</sup> and Tewfik Sari<sup>2\*</sup>

<sup>1</sup>MISTEA, Univ Montpellier, INRAE, Institut Agro, Montpellier,  
France.

<sup>2\*</sup>ITAP, Univ Montpellier, INRAE, Institut Agro, Montpellier,  
France.

<sup>3</sup>Laboratoire de Mathématiques, Université d'Avignon, France.

\*Corresponding author(s). E-mail(s): [tewfik.sari@inrae.fr](mailto:tewfik.sari@inrae.fr);

Contributing authors: [daliyoucef.manel@gmail.com](mailto:daliyoucef.manel@gmail.com);

[alain.rapaport@inrae.fr](mailto:alain.rapaport@inrae.fr);

## Abstract

The present work considers the model of two chemostats in series when a biomass mortality is considered in each vessel. We study the performance of the serial configuration for two different criteria which are the output substrate concentration and the biogas flow rate production, at steady state. A comparison is made with a single chemostat with the same total volume. Our techniques apply for a large class of growth functions and allow us to retrieve known results obtained when the mortality is not included in the model and the results obtained for specific growth functions in both the mathematical literature and the biological literature. In particular, we provide a complete characterization of operating conditions under which the serial configuration is more efficient than the single chemostat, i.e. the output substrate concentration of the serial configuration is smaller than that of the single chemostat or, equivalently, the biogas flow rate of the serial configuration is larger than that of the single chemostat. The study shows that the maximum biogas flow rate, relative to the dilution rate, of the series device is higher than that of the single chemostat provided that the volume of the first tank is large enough. This non-intuitive property does not occur for the model without mortality.

**Keywords:** chemostat, gradostat, mortality, bifurcations, global stability, operating diagram, biogas production

34 

## 1 Introduction

35 The mathematical model of the chemostat has received a great attention in the  
36 literature for many years (see for instance [16] and literature cited inside). This  
37 is probably due to its relative simplicity that can explain and predict quite  
38 faithfully the dynamics of real bioprocesses exploiting microbial ecosystems. It  
39 is today an important tool for decision making in industrial world, such as for  
40 dimensioning bioreactors or designing efficient operating conditions [13, 20].

41 Several extensions of the original model of the chemostat, considering spa-  
42 tial heterogeneity, have been proposed to better cope reality (see for instance  
43 [19]). Lovitt and Wimpenny has proposed the "gradostat" experimental device  
44 as a collection of chemostats of same volume interconnected in series [22, 23],  
45 which has led to the so-called "gradostat model" representing in a more gen-  
46 eral framework a gradient of concentrations [37, 40]. The gradostat model has  
47 been further generalized as the "general gradostat model" representing more  
48 general interconnection graphs with tanks of different volumes [38, 39].

49 Efficient use of a chemostat in practice relies on the analysis of its per-  
50 formance. The performance is considered for different criteria studied in the  
51 literature [31], among which the most common are: the output substrate  
52 concentration, the residence time, the biogas flow rate and the biomass pro-  
53 ductivity. Particular interconnection structures have been investigated and  
54 compared for the properties in terms of input-output performances (see for  
55 instance [5, 7, 15, 28]). It has been notably shown that a series of reactors  
56 instead of a single perfectly mixed one can significantly improve the perfor-  
57 mances of the bioprocess (in terms of matter conversion) while preserving  
58 the same residence time, or equivalently that the same performance can be  
59 obtained with a smaller residence time considering several tanks in series  
60 instead of a single one [14, 17, 24, 25, 47].

61 On another hand, it is known that in real processes, various growth con-  
62 ditions can be met and that it could be difficult to setup exactly the same  
63 perfect conditions in different reactors. These conditions include toxicity lev-  
64 els of culture media, which means more concretely that the consideration of  
65 a bacterial mortality, although often neglected compared to the removal rate,  
66 might be non avoidable and could also be variable. To the best of our knowl-  
67 edge, the possible impacts of mortality in the design of series of chemostats  
68 has not been yet studied in the literature, which is the purpose of the present  
69 work. Its contributions also cover interests in theoretical ecology for a better  
70 grasp of the interplay between spatial heterogeneity and mortality in resource-  
71 consumers models. Indeed, considering different removal rates in the classical  
72 chemostat model or more general ones allows to consider additional mortal-  
73 ity terms [21, 29, 34, 44]. However, these mathematical studies have mainly

concern analyses of equilibria and stability and not the performances of the system in presence of mortality.

In view of providing clear messages to the practitioners, we investigate how the operating diagram of a series of two interconnected chemostats in series is modified when considering different or identical mortality rates in both tanks. Operating diagrams have proven to be a good synthetic tool to summarize the possible operating modes, emphasized in [26] for its importance for bioreactors. Indeed, such diagrams are more and more often constructed both in the biological literature [26, 36, 41, 45] and the mathematical literature [1, 2, 4, 9–12, 18, 31–33, 35, 42, 43].

Then, we study the performances in terms of conversion ratio and byproduct production (such as biogas). As we shall see, several aspects are not intuitive, which show that the consideration of mortality can significantly modify the favorable operating conditions.

Along the paper, we use the abbreviations LES for locally exponentially stable and GAS for globally asymptotically stable in the positive orthant.

The paper is organized as follows. Section 2 includes the introduction of the mathematical model corresponding to the serial configuration of two chemostats with mortality rate. Afterwards, Section 3 focuses on the study of performances of the serial configuration with respect of the output substrate concentration. Then, Section 4 considers the performances of the serial configuration with respect of the biogas production. Next, Section 5 is devoted to illustrations and numerical simulations and a conclusion is given in Section 6. Moreover, we set up the single chemostat with mortality in Appendix A, while Appendix B is devoted to the existence and stability analysis of the steady states of the serial chemostat and Appendix C to its operating diagram. These results are extension of former results, in the case without mortality [7], but that have required to revisit significantly the mathematical proofs. Finally, Appendix D contains technical proofs.

## 2 Presentation of the model

We consider two serial interconnected chemostats where the total volume  $V$  is divided into  $V_1 = rV$  and  $V_2 = (1 - r)V$ , with  $r \in (0, 1)$ , as shown in Fig. 1. The substrate and the biomass concentrations in the tank  $i$  are respectively denoted  $S_i$  and  $x_i$ ,  $i = 1, 2$ . The input substrate concentration in the first chemostat is designated  $S^{in}$ , the flow rate is constant and is designated by  $Q$ . The output substrate concentration is the concentration of substrate in the second tank  $S^{out} = S_2$ .

The mathematical model is given by the following equations:

## 4 Performance study of two serial interconnected chemostats

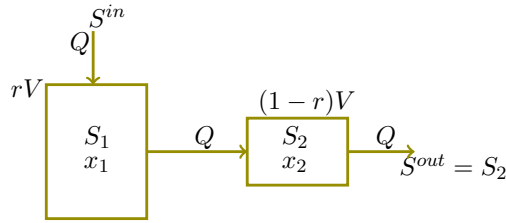


**Fig. 1** The serial configuration of two chemostats respectively of volumes  $rV$  and  $(1-r)V$ .

$$\begin{aligned}
 \dot{S}_1 &= \frac{D}{r}(S^{in} - S_1) - f(S_1)x_1 \\
 \dot{x}_1 &= -\frac{D}{r}x_1 + f(S_1)x_1 - ax_1 \\
 \dot{S}_2 &= \frac{D}{1-r}(S_1 - S_2) - f(S_2)x_2 \\
 \dot{x}_2 &= \frac{D}{1-r}(x_1 - x_2) + f(S_2)x_2 - ax_2,
 \end{aligned} \tag{1}$$

112 where  $\dot{S}_i = \frac{dS_i}{dt}$ ,  $\dot{x}_i = \frac{dx_i}{dt}$ ,  $i = 1, 2$ ,  $f$  is the growth function such that  $f(S_i)$   
 113 is the growth function of the substrate in the tank  $i = 1, 2$ ,  $a$  is the mortality  
 114 rate of the biomass and  $D = Q/V$  is the dilution rate of the whole structure.  
 115 The dilution rate of the first tank is  $Q/V_1 = D/r$ . The dilution rate of the  
 116 second tank is  $Q/V_2 = D/(1-r)$ .

117 Note that these equations are not valid for  $r = 0$  and  $r = 1$ , which corre-  
 118 spond to a single chemostat. For sake of completeness, the useful results on  
 119 the single chemostat are given in Appendix A. The considered growth function  
 120 satisfies the following properties.

121 **Assumption 1** The function  $f$  is  $C^1$ , with  $f(0) = 0$  and  $f'(S) > 0$  for all  $S > 0$ .

We define

$$m := \sup_{S>0} f(S), \quad (m \text{ may be } +\infty). \tag{2}$$

122 As  $f$  is increasing then the *break-even concentration* is defined by

$$\lambda(D) := f^{-1}(D) \quad \text{when } 0 \leq D < m. \tag{3}$$

123 The particular case without mortality of the biomass ( $a = 0$ ) is studied in  
 124 [7]. The results on the existence and stability of steady states of system (1) are  
 125 very similar to the case without mortality. The details are given in Appendix  
 126 B. The system can have up to three steady states:

- 127 • The washout steady state  $E_0 = (S^{in}, 0, S^{in}, 0)$ .
- 128 • The steady state  $E_1 = (S^{in}, 0, \bar{S}_2, \bar{x}_2)$  of washout in the first chemostat but  
 129 not in the second one.
- 130 • The steady state  $E_2 = (S_1^*, x_1^*, S_2^*, x_2^*)$  of persistence of the species in both  
 131 chemostats.

132 As in the case without mortality, see Table C2 in the Appendix, for any  
 133 operating condition  $(S^{in}, D)$ , one and only one of the steady-states  $E_0$ ,  $E_1$  and  
 134  $E_2$ , is stable. It is then globally asymptotically stable (GAS).

135 The operating diagram of the system is described in Appendix C. The  
 136 operating diagram has as coordinates the input substrate concentration  $S^{in}$   
 137 and the dilution rate  $D$ , and shows how the solutions of the system behave for  
 138 different values of these two parameters. The regions constituting the oper-  
 139 ating diagram correspond to different qualitative asymptotic behaviors. The  
 140 operating diagram of system (1) is depicted in Fig. 2.

141 The aim of this work is to establish a comparison of the performance of  
 142 the serial configuration with ones of the single chemostat. In the following,  
 143 we compare both structures according to two different criteria; the output  
 144 substrate concentration and the biogas flow rate.

### 145 3 Output substrate concentration

146 The output substrate concentration measures the biodegradation of the input  
 147 substrate by the overall device. The reduction of the output substrate concen-  
 148 tration is one of the main objectives of the biological wastewater treatment,  
 149 and its minimization is often addressed in the literature, see for example [46].  
 150 We assume that the serial configuration is functioning at a stable steady state.  
 151 The output substrate concentration at steady state depends on the parameters  
 152  $D$ ,  $S^{in}$  and  $r$ , and will be denoted  $S_r^{out}(S^{in}, D)$ .

153 **Proposition 1** Assume that Assumption 1 is satisfied. The output substrate con-  
 154 centration at steady state of system (1) is given by

$$S_r^{out}(S^{in}, D) = \begin{cases} S^{in} & \text{if } S^{in} \leq \min\left(\lambda\left(\frac{D}{1-r} + a\right), \lambda\left(\frac{D}{r} + a\right)\right) \\ \bar{S}_2 & \text{if } \lambda\left(\frac{D}{1-r} + a\right) \leq S^{in} \leq \lambda\left(\frac{D}{r} + a\right) \\ S_2^* & \text{if } S^{in} > \lambda\left(\frac{D}{r} + a\right) \end{cases} \quad (4)$$

155 where  $\bar{S}_2 = \lambda\left(\frac{D}{1-r} + a\right)$  and  $S_2^*$  is the unique solution of equation  $h(S_2) = f(S_2)$ .  
 156 In this equation, the function  $h$  is defined by:

$$h(S_2) = \frac{D+(1-r)a}{1-r} \frac{S_1^* - S_2}{b - S_2}, \quad (5)$$

157 where  $S_1^* = \lambda\left(\frac{D}{r} + a\right)$  and  $b = \frac{D(S^{in} - S_1^*)}{D + ra} + S_1^*$ .

158 *Proof* The output substrate concentration at steady state of system (1) is equal to  
 159  $S^{in}$ , if  $E_0$  is the GAS steady state. It is equal to  $\bar{S}_2$  if  $E_1$  is the GAS steady state  
 160 and to  $S_2^*$  if  $E_2$  is GAS. According to Theorem 3 in the Appendix,  $E_0$  is GAS if and  
 161 only if

$$D \geq \max(r, 1 - r)(f(S^{in}) - a),$$

6 *Performance study of two serial interconnected chemostats*

162 which is equivalent to

$$S^{in} \leq \min \left( \lambda \left( \frac{D}{1-r} + a \right), \lambda \left( \frac{D}{r} + a \right) \right).$$

163 On the other hand, using Theorem 3,  $\bar{S}_2$  depends on  $D$  and  $r$  and we have  
 164  $\bar{S}_2 = \lambda \left( \frac{D}{1-r} + a \right)$ .  $E_1$  is GAS if and only if

$$r(f(S^{in}) - a) \leq D \leq (1-r)(f(S^{in}) - a),$$

165 which is equivalent to

$$\lambda \left( \frac{D}{1-r} + a \right) \leq S^{in} \leq \lambda \left( \frac{D}{r} + a \right).$$

166 Finally, using Theorem 3, we know that  $S_2^*$  depends on parameters  $S^{in}$ ,  $D$ ,  $r$ . It  
 167 is the unique solution of equation  $h(S_2) = f(S_2)$ , where  $h$  is defined by (5). On the  
 168 other hand  $E_2$  is GAS if and only if the condition  $D < r(f(S^{in}) - a)$  is satisfied,  
 169 which is equivalent to the condition  $S^{in} > \lambda \left( \frac{D}{r} + a \right)$ .  $\square$

170 Although  $S_r^{out}(S^{in}, D)$  is defined only for  $0 < r < 1$ , we can extend it, by  
 171 continuity, for  $r = 0$  and  $r = 1$  by

$$S_0^{out}(S^{in}, D) = S_1^{out}(S^{in}, D) = S^{out}(S^{in}, D). \quad (6)$$

172 where  $S^{out}(S^{in}, D)$ , which is the output substrate concentration of the single  
 173 chemostat, is given by

$$S^{out}(S^{in}, D) = \begin{cases} S^{in} & \text{if } S^{in} \leq \lambda(D + a), \\ \lambda(D + a) & \text{if } S^{in} > \lambda(D + a). \end{cases} \quad (7)$$

174 For more information on  $S^{out}(S^{in}, D)$ , see Appendix A.

175 The proof of (6), comes from the following remarks. First, we have  
 176  $\bar{S}_2(D, 0) = \lambda(D + a)$  and second, according to Lemma 9 in the Appendix, we  
 177 can extend  $S_2^*(S^{in}, D, r)$ , by continuity, to  $r = 1$ , by

$$S_2^*(S^{in}, D, 1) = \lambda(D + a).$$

178 Our aim in this section is to compare  $S_r^{out}$  defined by (4) and (6) and  $S^{out}$   
 179 defined by (7).

### 180 3.1 The serial configuration can be more efficient than 181 the single chemostat

182 We fix  $r$  and we describe the set of operating conditions  $(S^{in}, D)$  for which

$$S_r^{out}(S^{in}, D) < S^{out}(S^{in}, D), \quad (8)$$

183 that is to say, the serial configuration with volumes  $rV$  and  $(1-r)V$ , is more  
 184 efficient than the single chemostat of volume  $V$ . For  $r \in (0, 1)$ , let  $g_r : [0, r(m -$   
 185  $a)) \mapsto \mathbb{R}$  defined by

$$g_r(D) := \lambda \left( \frac{D}{r} + a \right) + \frac{r(D+ar)}{(1-r)(D+a)} \left( \lambda \left( \frac{D}{r} + a \right) - \lambda(D + a) \right). \quad (9)$$

186 **Lemma 1** For  $r \in (0, 1)$  we have  $g_r(D) > \lambda\left(\frac{D}{r} + a\right)$ .

187 *Proof* As  $0 < r < 1$  and  $\lambda$  is an increasing function then, we have  $\lambda(D/r + a) >$   
 188  $\lambda(D + a)$ . Using (9), we have  $g_r(D) > \lambda(D/r + a)$ .  $\square$

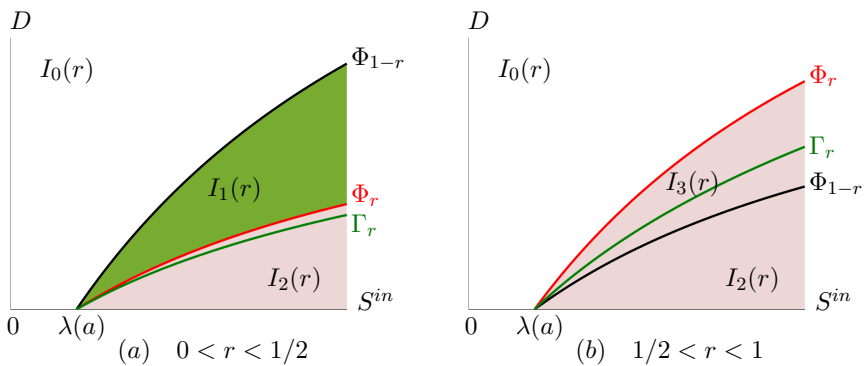


**Fig. 2** The operating diagram of of system (1) and the curve  $\Gamma_r$  defined by (14) under which the serial configuration is more efficient than the single chemostat.

189 **Theorem 1** Assume that Assumption 1 is satisfied. For any  $r \in (0, 1)$ , we have

$$S_r^{out}(S^{in}, D) = S^{out}(S^{in}, D) \iff S^{in} = g_r(D).$$

190 Moreover,

$$S_r^{out}(S^{in}, D) < S^{out}(S^{in}, D) \iff S^{in} > g_r(D).$$

191 *Proof* Recall that  $S_2^*(S^{in}, D, r)$  is the unique solution of equation  $f(S_2) = h(S_2)$   
 192 with  $h$  defined by (5). Let us first prove that

$$S_2^*(S^{in}, D, r) < \lambda(D + a) \iff S^{in} > g_r(D). \quad (10)$$

193 Since  $f$  is increasing, see Assumption 1, and  $h$  is decreasing, see Lemma 8 in the  
 194 Appendix, then the condition  $S_2^*(S^{in}, D, r) < \lambda(D + a)$  is equivalent to the condition  
 195  $h(\lambda(D + a)) < f(\lambda(D + a)) = D + a$ . Using (5), a straightforward computation shows  
 196 that the condition  $h(\lambda(D + a)) < D + a$  is equivalent to  $S^{in} > g_r(D)$ , where  $g_r$  is  
 197 defined by (9). This proves (10).

198 Let us go now to the proof of the theorem. Assume that  $S^{in} > g_r(D)$ . Using Lemma  
 199 1, we have

$$S^{in} > \lambda(D/r + a) > \lambda(D + a).$$

200 Using (4) and (7), we have



## 8 Performance study of two serial interconnected chemostats

$$\begin{aligned} S_r^{out}(S^{in}, D) &= S_2^*(S^{in}, D, r), \\ S^{out}(S^{in}, D) &= \lambda(D + a). \end{aligned} \quad (11)$$

From (10), we have  $S_r^{out}(S^{in}, D) < S^{out}(S^{in}, D)$ . Hence, we proved the following implication

$$S^{in} > g_r(D) \implies S_r^{out}(S^{in}, D) < S^{out}(S^{in}, D). \quad (12)$$

Assume now that  $S^{in} \leq g_r(D)$ . When  $r < 1/2$ , three cases must be distinguished. First, if

$$\lambda(D + a) < \lambda\left(\frac{D}{r} + a\right) < S^{in} \leq g_r(D),$$

then, by (4) and (7), we obtain (11). Hence, using (10), we have  $S_r^{out}(S^{in}, D) \geq S^{out}(S^{in}, D)$ . Secondly, if

$$\lambda(D + a) < \lambda\left(\frac{D}{1-r} + a\right) \leq S^{in} \leq \lambda\left(\frac{D}{r} + a\right),$$

then, by (4) and (7), we have

$$\begin{aligned} S_r^{out}(S^{in}, D) &= \lambda\left(\frac{D}{1-r} + a\right), \\ S^{out}(S^{in}, D) &= \lambda(D + a). \end{aligned}$$

Therefore, we have  $S_r^{out}(S^{in}, D) > S^{out}(S^{in}, D)$ . Finally, if  $S^{in} \leq \lambda(D + a)$ , then

$$S_r^{out}(S^{in}, D) = S^{out}(S^{in}, D) = S^{in}.$$

When  $r \geq 1/2$ , the proof is similar, excepted that we must distinguish only two cases,  $\lambda(D + a) < S^{in} \leq \lambda(D/r + a)$  and  $S^{in} \leq \lambda(D + a)$ . Hence, we have proved the reciprocal implication of (12). This completes the proof of second equivalence in the theorem.

The same calculations show the equivalence if inequalities are replaced by equalities.  $\square$

Theorem 1 asserts that the serial configuration is more efficient than the single chemostat if and only if  $S^{in} > g_r(D)$ . Let us illustrate this result in the operating diagram of system (1). Consider the curve of equation

$$\Phi_r = \{(S^{in}, D) : S^{in} = \lambda(D/r + a)\}. \quad (13)$$

According to the results given in Appendix C, the curves  $\Phi_r$  and  $\Phi_{1-r}$  defined by (13) separate the operating plane  $(S^{in}, D)$  in four regions in which the system has different asymptotic behaviour, see Table C2. To put it simply, in the  $I_0(r)$  region,  $E_0$  is GAS, in  $I_1(r)$ ,  $E_1$  is GAS, and in  $I_2(r) \cap I_3(r)$ ,  $E_3$  is GAS, see Fig. 2. This figure also shows the plot of the curve  $\Gamma_r$ , defined by

$$\Gamma_r := \{(S^{in}, D) : S^{in} = g_r(D)\}. \quad (14)$$

Using Lemma 1, we see that for all  $r \in (0, 1)$ , the curve  $\Gamma_r$  is always at right of the curve  $\Phi_r$ . According to Theorem 1, the output substrate concentration of the serial configuration is smaller than the one of the single chemostat, if and only if  $(S^{in}, D)$  is at right of the curve  $\Gamma_r$  depicted in Fig. 2.

## 3.2 The output substrate concentration as a function of the volume fraction $r$

In this section we assume that  $(S^{in}, D)$  is fixed and we look at the values of  $r$  for which (8) holds. More precisely we are going to describe the function

$$r \mapsto S_r^{out}(S^{in}, D). \quad (15)$$

**Proposition 2** *Assume that Assumption 1 is satisfied. Let  $D > 0$ ,  $S^{in} > \lambda(a)$ . We denote  $r_0 = D/(f(S^{in}) - a)$ .*

1. *If  $S^{in} \leq \lambda(D + a)$ , then for any  $r \in [0, 1]$ , one has  $S_r^{out}(S^{in}, D) = S^{out}(S^{in}, D) = S^{in}$ .*
2. *If  $\lambda(D + a) < S^{in} < \lambda(2D + a)$ , then  $1/2 < r_0 < 1$  and one has*

$$S_r^{out}(S^{in}, D) = \begin{cases} \bar{S}_2 & \text{if } 0 \leq r \leq 1 - r_0 \\ S^{in} & \text{if } 1 - r_0 \leq r \leq r_0 \\ S_2^* & \text{if } r_0 \leq r \leq 1. \end{cases} \quad (16)$$

3. *If  $\lambda(2D + a) \leq S^{in}$ , then  $0 < r_0 \leq 1/2$  and one has*

$$S_r^{out}(S^{in}, D) = \begin{cases} \bar{S}_2 & \text{if } 0 \leq r \leq r_0 \\ S_2^* & \text{if } r_0 \leq r \leq 1. \end{cases} \quad (17)$$

Here  $\bar{S}_2 = \lambda\left(\frac{D}{1-r} + a\right)$  and  $S_2^* = S_2^*(S^{in}, D, r)$  is the unique solution of equation  $f(S_2) = h(S_2)$ , where  $h$  is defined by (5).

*Proof* If  $S^{in} \leq \lambda(D + a)$ , then, for all  $r \in (0, 1)$ , one has

$$S^{in} \leq \lambda(D + a) \leq \min\left\{\lambda\left(\frac{D}{1-r} + a\right), \lambda\left(\frac{D}{r} + a\right)\right\}.$$

Then, according to (4), one has  $S_r^{out}(S^{in}, D) = S^{in}$ . This proves item 1 of the proposition.

Let  $r_0 = D/(f(S^{in}) - a)$ , i.e.  $S^{in} = \lambda(D/r_0 + a)$ .

If  $\lambda(D + a) < S^{in} < \lambda(2D + a)$ , then  $r_0 \in (1/2, 1)$ , so that  $1 - r_0 < r_0$ . The interval  $[0, 1]$  is subdivided into three sub-intervals. Firstly, if  $0 \leq r \leq 1 - r_0 < r_0$ , then  $r < r_0 \leq 1 - r$ , so that

$$\lambda\left(\frac{D}{1-r} + a\right) \leq S^{in} = \lambda\left(\frac{D}{r_0} + a\right) < \lambda\left(\frac{D}{r} + a\right).$$

Hence, according to (4), one has

$$S_r^{out}(S^{in}, D) = \lambda\left(\frac{D}{1-r} + a\right).$$

Secondly, if  $1 - r_0 \leq r \leq r_0$ , then  $r_0 \geq \max\{r, 1 - r\}$ , so that

$$S^{in} = \lambda\left(\frac{D}{r_0} + a\right) \leq \min\left\{\lambda\left(\frac{D}{1-r} + a\right), \lambda\left(\frac{D}{r} + a\right)\right\}.$$

Hence, according to (4), one has  $S_r^{out}(S^{in}, D) = S^{in}$ . Finally, if  $r_0 < r \leq 1$ , then one has

$$S^{in} = \lambda\left(\frac{D}{r_0} + a\right) > \lambda\left(\frac{D}{r} + a\right).$$

Hence, according to (4), one has

$$S_r^{out}(S^{in}, D) = S_2^*(S^{in}, D, r).$$

This proves item 2 of the proposition.

If  $\lambda(2D + a) \leq S^{in}$ , then  $r_0 \in (0, 1/2]$ . Therefore,  $r_0 \leq 1 - r_0$ . The proof of item 3 of the proposition is the same as the proof of item 2 excepted that now, the interval  $[0, 1]$  is subdivided now into two sub-intervals  $[0, r_0]$  and  $[r_0, 1]$ , so that the interval for which  $S_r^{out}(S^{in}, D) = S^{in}$  is empty.  $\square$

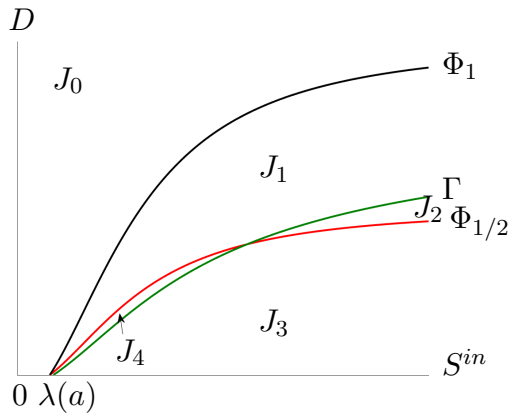


**Fig. 3** In each region  $J_i$ ,  $i = 0, \dots, 4$ , the map  $r \mapsto S_r^{out}(S^{in}, D)$  for fixed  $(S^{in}, D)$  has a different behavior.

We want to determine the values  $r \in (0, 1)$  for which the condition (8) is satisfied. We need the following Assumption that is satisfied by any concave growth function but also by non concave growth functions, satisfying additional conditions, see Section 3.4.

**Assumption 2** For every  $D \in [0, m - a)$ , the function  $r \in (D/(m - a), 1) \mapsto g_r(D) \in \mathbb{R}$  is decreasing.

Let  $D < m - a$ . Using  $g_r(D) > \lambda(D/r + a)$ , we have

$$\lim_{r \rightarrow D/(m-a)} g_r(D) > \lim_{r \rightarrow D/(m-a)} \lambda(D/r + a) = +\infty.$$

On the other hand, using L'Hôpital's rule, we have

$$\lim_{r \rightarrow 1} g_r(D) = g(D). \quad (18)$$

261 where  $g : [0, m - a) \rightarrow \mathbb{R}^+$  is defined by

$$g(D) = \lambda(D + a) + D\lambda'(D + a). \quad (19)$$

262 Therefore, from Assumption 2, the function  $r \mapsto g_r(D)$  is decreasing from  
263  $(D/(m - a), 1)$  to  $(g(D), +\infty)$ . Hence, it admits an inverse function

$$S^{in} \in (g(D), +\infty) \mapsto r_1(S^{in}, D) \in (D/(m - a), 1).$$

264 We use the notation  $r_1(\cdot, D)$  to recall the dependence of the inverse function  
265 in  $D$ . For all  $D \in (0, m - a)$ ,  $r \in (D/(m - a), 1)$  and  $S^{in} > g(D)$ , we have

$$r = r_1(S^{in}, D) \iff S^{in} = g_r(D), \quad (20)$$

$$r > r_1(S^{in}, D) \iff S^{in} > g_r(D). \quad (21)$$

266 **Theorem 2** Assume that Assumptions 1 and 2 are satisfied. Let  $g$  defined by (19).

- 267 • If  $S^{in} \leq g(D)$  then for any  $r \in (0, 1)$ , we have  $S_r^{out}(S^{in}, D) > S^{out}(S^{in}, D)$ .
- 268 In addition, for  $r = 0$  and  $r = 1$  we have  $S_r^{out}(S^{in}, D) = S^{out}(S^{in}, D)$ .
- 269 • If  $S^{in} > g(D)$  then  $S_r^{out}(S^{in}, D) < S^{out}(S^{in}, D)$  if and only if  $r_1(S^{in}, D) <$   
270  $r < 1$ , with  $r_1(S^{in}, D)$ , defined by (20). In addition, for  $r = 0$ ,  $r =$   
271  $r_1(S^{in}, D)$  and  $r = 1$ , we have  $S_r^{out}(S^{in}, D) = S^{out}(S^{in}, D)$ .

272 *Proof* The function  $r \mapsto g_r(D)$  is decreasing and tends to  $g(D)$  as  $r$  tends to 1, as  
273 shown by (18). Thus, for all  $r \in (0, 1)$ , we have  $g(D) < g_r(D)$ . If  $S^{in} \leq g(D)$ , then  
274  $S^{in} < g_r(D)$ . According to Theorem 1, for all  $r \in (0, 1)$ , we have  $S_r^{out}(S^{in}, D) >$   
275  $S^{out}(S^{in}, D)$ .

276 Let  $S^{in} > g(D)$ . Let  $r_1 = r_1(S^{in}, D)$ . According to (21), for all  $r > r_1$ , we have  
277  $S^{in} > g_r(D)$ . Thus, according to Theorem 1, we have  $S_r^{out}(S^{in}, D) < S^{out}(S^{in}, D)$ .

278 The equality  $S_r^{out}(S^{in}, D) = S^{out}(S^{in}, D)$  is verified for the  $r = 0$  and  $r = 1$ , see  
279 (6). In addition, we have  $S^{in} = g_{r_1}(D)$ , see (20). Hence, according to Theorem 1, we  
280 have  $S_{r_1}^{out}(S^{in}, D) = S^{out}(S^{in}, D)$ .  $\square$

281 Let us now describe the subsets of the operational space  $(S^{in}, D)$  for which  
282 the behaviour described in the three cases of Proposition 2 occurs. For a complete  
283 description we will also distinguish the sub-cases for which there exists  
284  $r_1 = r_1(S^{in}, D)$  such that, for  $r_1 < r < 1$ , (8) is satisfied, as shown in Theorem  
285 2. Consider the curves  $\Phi_1$  and  $\Phi_{1/2}$ , defined by (13), and the curve  $\Gamma$  defined  
286 by

$$\Gamma := \{(S^{in}, D) : S^{in} = g(D)\}, \quad (22)$$

287 These three curves intersect at  $(\lambda(a), 0)$  and, using the inequality  $g(D) >$   
288  $\lambda(D + a)$ , which is satisfied for all  $D > 0$ , one deduces that  $\Gamma$  is at the right

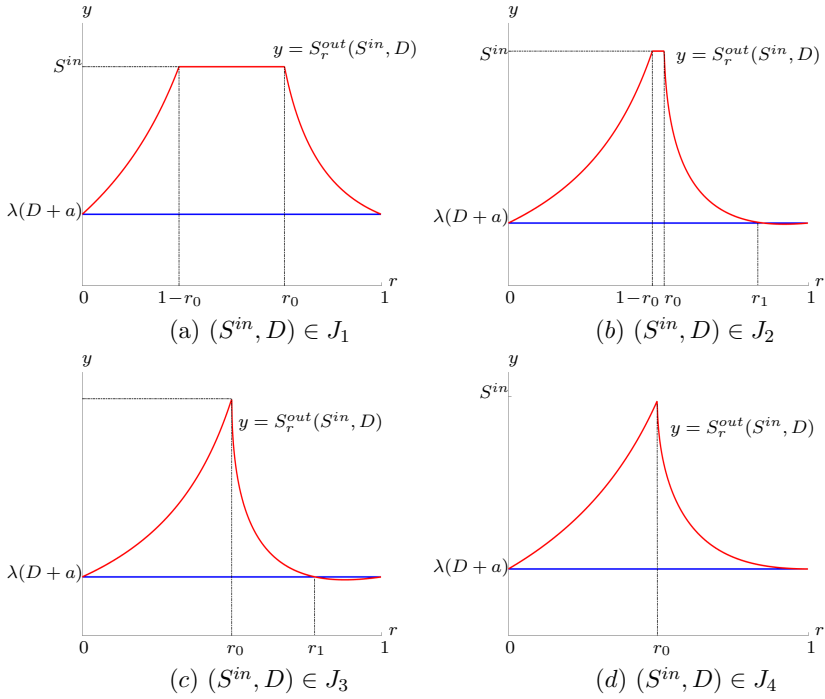


**Fig. 4** For  $S^{in}$  and  $D$  fixed, the output substrate concentration of the serial configuration, in red, compared to that of the single chemostat, in blue;  $r_1(S^{in}, D)$  is defined by (20),  $r_0 = D/(f(S^{in}) - a)$  and  $J_1, J_2, J_3, J_4$  are depicted in Fig. 3.

289 of  $\Phi_1$ . Therefore, the curves  $\Phi_1, \Phi_{1/2}$  and  $\Gamma$  separate the set of operating  
 290 parameters  $(S^{in}, D)$  into the following four subsets, see Fig. 3.

$$\begin{aligned}
 J_0 &= \{(S^{in}, D) : S^{in} \leq \lambda(2D + a)\}, \\
 J_1 &= \{(S^{in}, D) : \lambda(D + a) < S^{in} \leq \min\{g(D), \lambda(2D + a)\}\}, \\
 J_2 &= \{(S^{in}, D) : g(D) < S^{in} < \lambda(2D + a)\}, \\
 J_3 &= \{(S^{in}, D) : \max\{g(D), \lambda(2D + a)\} \leq S^{in}\}, \\
 J_4 &= \{(S^{in}, D) : \lambda(2D + a) < S^{in} < g(D)\}.
 \end{aligned} \tag{23}$$

291 Combining the results of Proposition 2 and Theorem 2, we find that the  
 292 function  $r \mapsto S_r^{out}(S^{in}, D)$  is as in Fig. 4. In the following we will comment on  
 293 this figure.

- 294 • If  $(S^{in}, D) \in J_1$ , then when  $S^{in} < \lambda(2D + a)$ ,  $S_r^{out}(S^{in}, D)$  is given by (16)  
 295 and when  $S^{in} = \lambda(2D + a)$ ,  $S_r^{out}(S^{in}, D)$  is given by (17). In addition, for  
 296 all  $r \in (0, 1)$ ,  $S_r^{out}(S^{in}, D) > S^{out}(S^{in}, D)$ . The equality is fulfilled for  $r = 0$   
 297 and  $r = 1$ , see Fig. 4(a).
- 298 • If  $(S^{in}, D) \in J_2$ , then  $S_r^{out}(S^{in}, D)$  is given by (16) and  $S_r^{out}(S^{in}, D) <$   
 299  $S^{out}(S^{in}, D)$  if and only if  $r \in (r_1(S^{in}, D), 1)$ , where  $r_1(S^{in}, D)$  is defined

by (20). The equality is fulfilled for  $r = 0$ ,  $r = r_1(S^{in}, D)$  and  $r = 1$ , see Fig. 4(b).

- If  $(S^{in}, D) \in J_3$  then  $S_r^{out}(S^{in}, D)$  is given by (17) and  $S_r^{out}(S^{in}, D) < S^{out}(S^{in}, D)$  if and only if  $S^{in} > g(D)$  and  $r \in (r_1(S^{in}, D), 1)$  where  $r = r_1(S^{in}, D)$  is defined by (20). The equality is fulfilled for  $r = 0$ ,  $r = r_1(S^{in}, D)$  and  $r = 1$ , see Fig. 4(c).
- If  $(S^{in}, D) \in J_4$  then  $S_r^{out}(S^{in}, D)$  is given by (17) and for all  $r \in (0, 1)$ ,  $S_r^{out}(S^{in}, D) > S^{out}(S^{in}, D)$ . The equality is fulfilled for  $r = 0$  and  $r = 1$ , see Fig. 4(d).

Note that if  $(S^{in}, D) \in J_0$ , then case 1 of Proposition 2 occurs. One remarks that the lowest value of the red curve, corresponding to the lowest output substrate concentration of the serial configuration, is obtained for  $(S^{in}, D) \in J_2 \cap J_3$  and  $r > r_1(S^{in}, D)$ . This lowest concentration is obtained with the best possible serial configuration.

Figures 2, 3 and 4 are made without graduations on the axes because they represent general situations where the growth function is only assumed to verify our hypotheses. It should be noticed that regions  $J_0$ ,  $J_1$  and  $J_3$  always exist and are connected. However, regions the  $J_2$  and  $J_4$  do not always exist or are necessarily connected. This depends on the number of points of intersection between curves  $\Phi_{1/2}$  and  $\Gamma$ . For a linear growth rate,  $\Phi_{1/2} = \Gamma$  and hence, regions  $J_2$  and  $J_4$  do not exist, see Fig. 7(a). For a Monod growth function, curves  $\Phi_{1/2}$  and  $\Gamma$  intersect only at point  $(\lambda(a), 0)$  and hence, region  $J_3$  always exist and is connected but region  $J_3$  does not exist, see Fig. 8(a). For a Hill growth function, curves  $\Phi_{1/2}$  and  $\Gamma$  always intersect at  $(\lambda(a), 0)$  and also at a unique positive point, Lemma 6. Hence, regions  $J_2$  and  $J_4$  both exist and are connected, see Fig. 9(a,b,c).

### 3.3 The output substrate concentration as a function of the dilution rate

In this section we assume that  $S^{in}$  and  $r$  are fixed and we look at the values of the dilution rate  $D$  for which (8) holds, i.e. the serial configuration, is more efficient than the single chemostat. More precisely we are going to describe the function

$$D \mapsto S_r^{out}(S^{in}, D). \quad (24)$$

We want to determine the subset of values of  $D$  for which the condition (8) is satisfied. We need the following Assumption that is satisfied by any concave growth function, but also by non concave growth functions, satisfying additional conditions, see Section 3.4.

**Assumption 3** For every  $r \in (0, 1)$ , the function  $D \in [0, r(m - a)] \mapsto g_r(D) \in \mathbb{R}$  is increasing.

Using  $g_r(D) > \lambda(D/r + a)$ , we have

$$\lim_{D \rightarrow r(m-a)} g_r(D) > \lim_{D \rightarrow r(m-a)} \lambda(D/r + a) = +\infty.$$

From Assumption 3, the function  $D \mapsto g_r(D)$  is increasing from  $[0, r(m-a))$  to  $[g_r(0) = \lambda(a), +\infty)$ . Hence, it admits an inverse function

$$S^{in} \in (\lambda(a), +\infty) \mapsto D_r(S^{in}) \in [0, r(m-a)).$$

For all  $r \in (0, 1)$ ,  $S^{in} \geq \lambda(a)$  and  $D \in [0, r(m-a))$ , we have

$$D = D_r(S^{in}) \iff S^{in} = g_r(D), \quad (25)$$

$$D < D_r(S^{in}) \iff S^{in} > g_r(D). \quad (26)$$

**Proposition 3** Assume that Assumptions 1 and 3 are satisfied. We have

$$S_r^{out}(S^{in}, D) < S^{out}(S^{in}, D) \iff 0 < D < D_r(S^{in}),$$

338 where  $D_r(S^{in})$  is defined by (25).

339 *Proof* Let  $r \in (0, 1)$ . According to (26), if  $D < D_r(S^{in})$ , then  $S^{in} > g_r(D)$ . Conse-  
340 quently, according to Theorem 1, we have  $S_r^{out}(S^{in}, D) < S^{out}(S^{in}, D)$ .  $\square$

### 341 3.4 How to check Assumptions 2 and 3

342 In this section we give sufficient conditions for Assumption 2 and 3 to be  
343 satisfied. These conditions will be useful for the applications given in Section  
344 5. For this purpose we consider the function  $\gamma$  defined by

$$\gamma(r, D) = g_r(D), \quad (27)$$

defined on

$$\text{dom}(\gamma) = \{(r, D) : 0 < r < 1, 0 < D/r + a < m\},$$

345 which consists simply in considering  $g_r(D)$ , given by (9), as a function of both  
346 variables  $r$  and  $D$ . If

$$\frac{\partial \gamma}{\partial r}(r, D) < 0 \text{ for all } (r, D) \in \text{dom}(\gamma),$$

347 then Assumption 2 is satisfied. Similarly, if

$$\frac{\partial \gamma}{\partial D}(r, D) > 0 \text{ for all } (r, D) \in \text{dom}(\gamma),$$

348 then Assumption 3 is satisfied. The following Lemmas give sufficient condi-  
349 tions, for partial derivatives of  $\gamma$  to have their signs as indicated above.

350 **Lemma 2** For  $D \in (0, m - a)$ , let  $l_D$  be defined on  $\text{dom}(l_D) = (D/(m - a), 1]$  by  
 351  $l_D(r) = \lambda(D/r + a)$ .

a) Assume that for  $D \in (0, m - a)$  and  $r \in \text{dom}(l_D)$  we have

$$l_D(1) > l_D(r) + (1 - r)l'_D(r) \quad (28)$$

352 then, for all  $(r, D) \in \text{dom}(\gamma)$ , we have  $\frac{\partial \gamma}{\partial r}(r, D) < 0$ .

353 b) If, for  $D \in (0, m - a)$ ,  $l_D$  is strictly convex on  $\text{dom}(l_D)$ , then the condition (28)  
 354 is satisfied.

355 c) If  $f$  is twice derivable, then  $l_D$  is twice derivable and the following conditions are  
 356 equivalent

- 357 1. For  $D \in (0, m - a)$  and  $r \in \text{dom}(l_D)$ ,  $l''_D(r) > 0$ .
- 358 2. For  $S > \lambda(a)$ ,  $(f(S) - a)f''(S) < 2(f'(S))^2$ .

*Proof* Notice first that  $\gamma(r, D)$  can be written as follows

$$\begin{aligned} \gamma(r, D) &= g_r(D) = \lambda(D + a) + \\ &\quad \left( \frac{1}{1-r} - \frac{ra}{D+a} \right) \left( \lambda \left( \frac{D}{r} + a \right) - \lambda(D + a) \right). \end{aligned} \quad (29)$$

Using the definition of  $l_D$ ,  $\gamma(r, D)$  is given then by

$$\gamma(r, D) = l_D(1) + \left( \frac{1}{1-r} - \frac{ra}{D+a} \right) (l_D(r) - l_D(1)).$$

359 The partial derivative, with respect to  $r$  of  $\gamma$  is given then by

$$\begin{aligned} \frac{\partial \gamma}{\partial r}(r, D) &= \frac{a(1-2r)}{D+a} l'_D(r) + \\ &\quad \left( \frac{1}{(1-r)^2} - \frac{a}{D+a} \right) (l_D(r) - l_D(1) + (1-r)l'_D(r)). \end{aligned} \quad (30)$$

Notice that  $\frac{1}{(1-r)^2} - \frac{a}{D+a} > 0$  for all  $r \in (0, 1)$ . From  $l'_D(r) = -\frac{D}{r^2} \lambda' \left( \frac{D}{r} + a \right)$ , it is deduced that  $l'_D(r) < 0$ . Therefore, if the condition (28) is satisfied, and, in addition  $0 < r \leq 1/2$ , then, from (30), it is deduced that  $\frac{\partial \gamma}{\partial r}(r, D) < 0$ .

In the case  $r \in (1/2, 1)$ , we use the following expression of  $\gamma(r, D)$  which is deduced from (29):

$$\gamma(r, D) = l_D(1) + B(r) \frac{l_D(r) - l_D(1)}{1-r},$$

where  $B(r) = \frac{D+a-ar(1-r)}{D+a}$ . Straightforward computation show that

$$\frac{\partial \gamma}{\partial r}(r, D) = \frac{D+ar(2-r)}{(D+a)(1-r)^2} (l_D(r) - l_D(1) + (1-r)C(r)l'_D(r)), \quad (31)$$

where  $C(r) = \frac{D+a-ar(1-r)}{D+ar(2-r)}$ . We have

$$C'(r) = \frac{a}{(D+ar(2-r))^2} (ar^2 + 2(a + 2D)r - 3D - 2a).$$

360 Thus  $C'(r) = 0$  for

$$r = r^* := \frac{1}{a} \left( \sqrt{3a^2 + 7aD + 4D^2} - a - 2D \right) \in (1/2, 1)$$



and  $(r - r^*)C'(r) > 0$  for  $r \in (1/2, 1)$ ,  $r \neq r^*$ . Hence, from  $C(1/2) = C(1) = 1$ , we have  $0 < C(r) < 1$  for all  $r \in (1/2, 1)$ . Now, if we assume that (28) is satisfied, for  $1/2 < r < 1$  we have

$$l_D(1) > l_D(r) + (1 - r)l'_D(r) > l_D(r) + (1 - r)C(r)l'_D(r).$$

361 Hence, from (31), it is deduced that  $\frac{\partial \gamma}{\partial r}(r, D) < 0$ . This proves part *a* of the lemma.

Moreover, if  $l_D$  is strictly convex on  $\text{dom}(l_D)$  then for all  $s$  and  $r$  in  $(D/(m-a), 1]$ , if  $s \neq r$ , then

$$l_D(s) > l_D(r) + (s - r)l'_D(r).$$

Taking  $s = 1$  and  $r \in \text{dom}(l_D)$  one obtains the condition (28). This proves part *b* of the lemma. Assume now that  $f$ , and hence  $l_D$ , are twice derivable. Using

$$\lambda'(D) = \frac{1}{f'(\lambda(D))}, \quad \lambda''(D) = -\frac{f''(\lambda(D))}{(f'(\lambda(D)))^3}, \quad (32)$$

we can write

$$\begin{aligned} l''_D(r) &= \frac{2D}{r^3} \lambda' \left( \frac{D}{r} + a \right) + \frac{D^2}{r^4} \lambda'' \left( \frac{D}{r} + a \right) \\ &= \frac{D \left( 2 \left( f' \left( \lambda \left( \frac{D}{r} + a \right) \right) \right)^2 - \frac{D}{r} f'' \left( \lambda \left( \frac{D}{r} + a \right) \right) \right)}{r^3 \left( f' \left( \lambda \left( \frac{D}{r} + a \right) \right) \right)^3}. \end{aligned}$$

362 Therefore, the condition 1 in item *c* in the lemma is equivalent to the following  
363 condition: For all  $D \in (0, m - a)$  and  $r \in (D/(m - a), 1]$ , we have

$$\frac{D}{r} f'' \left( \lambda \left( \frac{D}{r} + a \right) \right) < 2 f' \left( \lambda \left( \frac{D}{r} + a \right) \right)^2. \quad (33)$$

364 Using the notation  $S = \lambda \left( \frac{D}{r} + a \right)$ , which is the same as  $D/r = f(S) - a$ , the  
365 condition (33) is equivalent to : For all  $S > 0$ ,  $(f(S) - a)f''(S) < 2(f'(S))^2$ , which  
366 is the condition 2 in *c* in the lemma.  $\square$

367 **Lemma 3** Assume that

$$f' \left( \lambda \left( \frac{D}{r} + a \right) \right) \leq \frac{1}{r} f'(\lambda(D + a)). \quad (34)$$

368 Then,  $\frac{\partial \gamma}{\partial D}(r, D) > 0$ . Hence Assumption 3 is satisfied. If  $f'$  is decreasing, then the  
369 condition (34) is satisfied.

370 *Proof* From (29) we deduce that

$$\begin{aligned} \frac{\partial \gamma}{\partial D}(r, D) &= \lambda'(D + a) + \frac{ra}{(D+a)^2} \left( \lambda \left( \frac{D}{r} + a \right) - \lambda(D + a) \right) \\ &\quad + \left( \frac{1}{1-r} - \frac{ra}{D+a} \right) \left( \frac{1}{r} \lambda' \left( \frac{D}{r} + a \right) - \lambda'(D + a) \right). \end{aligned}$$

371 Notice that  $\frac{1}{1-r} - \frac{ra}{D+a} > 0$ ,  $\lambda'(D + a) > 0$  and  $\lambda \left( \frac{D}{r} + a \right) > \lambda(D + a)$ . Therefore  
372 the condition

$$\frac{1}{r} \lambda' \left( \frac{D}{r} + a \right) - \lambda'(D + a) \geq 0$$

373 is sufficient to have  $\frac{\partial \gamma}{\partial D}(r, D) > 0$ . Using (32), this condition is equivalent to (34).  
374 Note that if  $f'$  is decreasing, then this condition is satisfied. Indeed, we have

$$f' \left( \lambda \left( \frac{D}{r} + a \right) \right) \leq f'(\lambda(D + a)) \leq \frac{1}{r} f'(\lambda(D + a)),$$

375 which is the condition (34).  $\square$

376 *Remark 1* Notice that:

377 *i)* The condition 2 in part c of Lemma 2 is equivalent to the condition

$$\text{For all } S > \lambda(a), \frac{d^2}{dS^2} \left( \frac{1}{f(S)-a} \right) > 0. \quad (35)$$

378 Therefore, if  $f$  satisfies the condition (35), then it verifies Assumption 2.

379 *ii)* If the increasing growth function  $f$  is twice derivable and satisfies  $f''(S) \leq 0$  for  
380 all  $S > 0$ , then the condition b in Lemma 2 and the condition (34) in Lemma 3  
381 are satisfied. Thus, Assumptions 2 and 3 are satisfied and our results apply for any  
382 concave growth function.

383 *iii)* Assume that the increasing growth function  $f$  is twice derivable and there exists  
384  $\hat{S} \in (0, +\infty)$  such that  $f''$  is nonnegative on  $(0, \hat{S})$  and nonpositive on  $(\hat{S}, +\infty)$ .  
385 If moreover the condition 2 in part c of Lemma 2 is verified for  $a = 0$ , then this  
386 condition is also verified for any  $a > 0$  and  $S \in (\lambda(a), \hat{S})$ . Therefore, if  $(1/f)'' > 0$   
387 on  $(0, \hat{S})$  then Assumption 2 is satisfied.

388 We will see in Section 5, how to use Remark 1 and Lemmas 2 and 3 to show  
389 that a linear growth function, a Monod function and a Hill function satisfy  
390 Assumptions 2 and 3.

## 391 4 Biogas flow rate

392 Microbial activity often produces by-products such as biogas, which can be  
393 a valuable source of energy in certain contexts. For instance, the anaerobic  
394 digestion of organic matter by microbial species produces methane and carbon  
395 dioxide. Valorizing biogas production while treating wastewater has received  
396 recently great attention, as a way of producing valuable energy and limiting  
397 the carbon footprint of the process [30].

398 We recall that the biogas flow rate is proportional to the microbial activity,  
399 as defined for instance in [3, 27]. We consider here the biogas flow rate as a  
400 function of the input substrate concentration  $S^{in}$ , the dilution rate  $D$  and the  
401 parameter  $r$ .

402 For  $r(f(S^{in}) - a) \leq D < (1 - r)(f(S^{in}) - a)$ , the biogas flow rate  
403 corresponding to the steady state  $E_1$  is given by the expression

$$G_1(S^{in}, D, r) = V_2 \bar{x}_2 f(\bar{S}_2), \quad (36)$$

404 with  $V_2 = (1 - r)V$ ,  $\bar{x}_2$  and  $\bar{S}_2$  defined in (B15).

405 For  $D < r(f(S^{in}) - a)$ , the biogas flow rate corresponding to the positive  
406 steady state  $E_2$  is given by the expression

$$G_2(S^{in}, D, r) = V_1 x_1^* f(S_1^*) + V_2 x_2^* f(S_2^*), \quad (37)$$

407 with  $V_1 = rV$ ,  $V_2 = (1 - r)V$ ,  $x_1^*$  and  $S_1^*$  defined in (B17),  $x_2^*$  defined by (B18)  
408 and  $S_2^*$  the unique solution of  $h(S_2) = f(S_2)$ .

**Proposition 4** 1. When  $r(f(S^{in}) - a) \leq D$  and  $D < (1 - r)(f(S^{in}) - a)$  then

$$G_1(S^{in}, D, r) = VD(S^{in} - \bar{S}_2). \quad (38)$$

2. When  $D < r(f(S^{in}) - a)$  then

$$G_2(S^{in}, D, r) = VD(S^{in} - S_2^*). \quad (39)$$

*Proof* From system (B10), considering equation  $\dot{S}_2 = 0$ , one obtains  $\bar{x}_2 f(\bar{S}_2) = D(S^{in} - \bar{S}_2)/(1 - r)$ . Thus,

$$G_1(S^{in}, D, r) = V_1 \frac{D}{r} (S^{in} - \bar{S}_2) = VD(S^{in} - \bar{S}_2).$$

From system (B10), considering  $\dot{S}_1 = 0$  and  $\dot{S}_2 = 0$  gives respectively  $x_1^* f(S_1^*) = D(S^{in} - S_1^*)/r$  and  $x_2^* f(S_2^*) = D(S_1^* - S_2^*)/(1 - r)$ . Thus, one has

$$\begin{aligned} G_2(S^{in}, D, r) &= V_1 \frac{D}{r} (S^{in} - S_1^*) + V_2 \frac{D}{1-r} (S_1^* - S_2^*) \\ &= VD(S^{in} - S_2^*). \end{aligned}$$

409 This ends the proof of the proposition.  $\square$

410 Although  $G_1(S^{in}, D, r)$  and  $G_2(S^{in}, D, r)$ , given by (36) and (37), respectively, are not defined for  $r = 0$  or  $r = 1$ , the formulas (38) and (39) allow them  
411 to be extended to  $r = 0$  and  $r = 1$ , as was done for  $S_r^{out}$  in (6). We can write  
412

$$G_1(S^{in}, D, 0) = G_2(S^{in}, D, 1) = G_{chem}(S^{in}, D),$$

where

$$G_{chem}(S^{in}, D) = VD(S^{in} - \lambda(D + a)), \quad (40)$$

413 represents the biogas flow rate of the single chemostat when  $0 < D < f(S^{in}) -$   
414  $a$ . For more information on  $G_{chem}(S^{in}, D)$ , see (A7) in Appendix A.

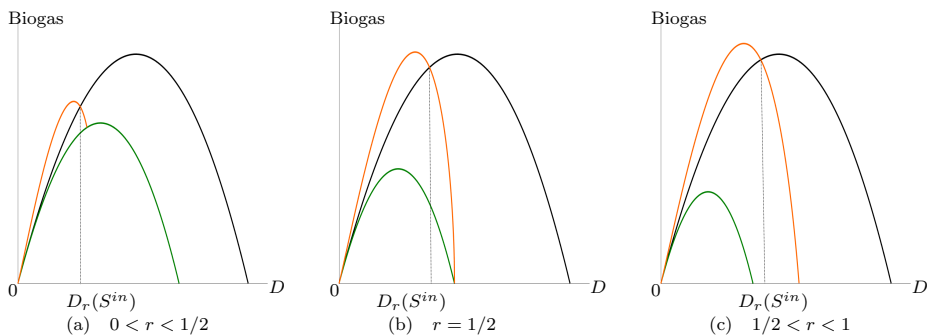


**Fig. 5** For  $r$  and  $S^{in}$  fixed, the curves of the maps  $D \mapsto G_1(S^{in}, D, r)$ , in green,  $D \mapsto G_2(S^{in}, D, r)$ , in orange, and  $D \mapsto G_{chem}(S^{in}, D)$ , in black, where  $G_1$ ,  $G_2$  and  $G_{chem}$  are given by (38), (39) and (40) respectively.

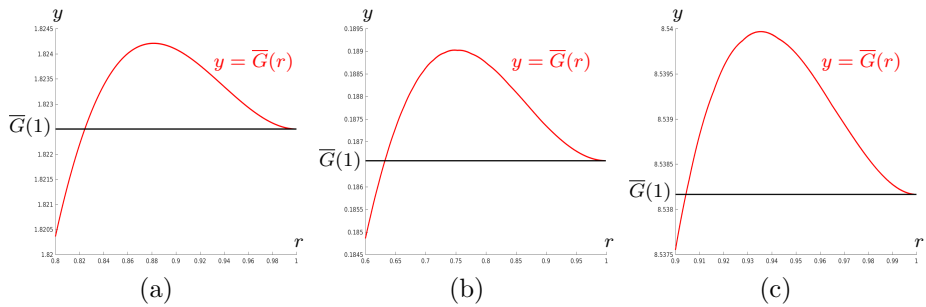


**Fig. 6** The map  $r \mapsto \overline{G}(r)$  with  $\overline{G}$  defined by (42). (a)  $f(S) = 4S$ ,  $a = 0.6$  and  $S^{in} = 1.5$ . (b)  $f(S) = 4S/(5 + S)$ ,  $a = 0.3$  and  $S^{in} = 1.5$ . (c)  $f(S) = 4S^2/(25 + S^2)$ ,  $a = 0.3$  and  $S^{in} = 10$ .

#### 4.1 The serial configuration can be more efficient than the single chemostat

In this section, we prove that the biogas flow rate  $G_1$  corresponding to the steady state  $E_1$  is always smaller than the biogas flow rate of the single chemostat. However, the biogas flow rate  $G_2$  corresponding to the steady state  $E_2$  can be larger than the biogas flow rate of the single chemostat. More precisely, we have the following result.

**Proposition 5** Assume that Assumption 1 is satisfied. Let  $r \in (0, 1)$ ,  $0 \leq D < f(S^{in}) - a$  and  $G_{chem}$  defined by (40).

1. If  $r(f(S^{in}) - a) \leq D$  and  $D < (1 - r)(f(S^{in}) - a)$ , then  $G_1(S^{in}, D, r) < G_{chem}(S^{in}, D)$ , where  $G_1$  is given by (38).
2. If  $D < r(f(S^{in}) - a)$ , then

$$G_2(S^{in}, D, r) > G_{chem}(S^{in}, D) \iff S^{in} > g_r(D),$$

where  $G_2$  is given by (39) and  $g_r$  is defined by (9).

- If, in addition, Assumption 2 is satisfied, and  $S^{in} > g(D)$ , then  $G_2(S^{in}, D, r) > G_{chem}(S^{in}, D)$ , if and only if  $r > r_1(S^{in}, D)$ , where  $r_1(S^{in}, D)$  is defined by (20).
- If, in addition, Assumption 3 is satisfied, then  $G_2(S^{in}, D, r) > G_{chem}(S^{in}, D)$ , if and only if  $D < D_r(S^{in})$ , where  $D_r(S^{in})$  is defined by (25).

*Proof 1.* Since  $D/(1 - r) > D$  and  $\lambda$  is increasing, we have  $\lambda(D/(1 - r) + a) > \lambda(D + a)$ . Then, using the formula for  $G_1$  given in Proposition 4, this induces the inequality  $G_1(S^{in}, D, r) < G_{chem}(S^{in}, D)$ .

436 2. According to Theorem 1, for any  $r \in (0, 1)$  and  $D < r(f(S^{in}) - a)$  one  
 437 has  $S_2^*(S^{in}, D, r) < \lambda(D + a)$  if and only if  $S^{in} > g_r(D)$ . Consequently,  
 438 using the formula for  $G_2$  given in Proposition 4, one has  $G_2(S^{in}, D, r) >$   
 439  $G_{chem}(S^{in}, D)$  if and only if  $S^{in} > g_r(D)$ . If Assumption 2 is satisfied,  
 440 then, using (21), we see that  $G_2(S^{in}, D, r) > G_{chem}(S^{in}, D)$  if and only if  
 441  $r > r_1(S^{in}, D)$ . If Assumption 3 is satisfied, then, using (26), we see that  
 442  $G_2(S^{in}, D, r) > G_{chem}(S^{in}, D)$  if and only if  $D < D_r(S^{in})$ .  
 443 This ends the proof of the proposition.  $\square$

444 Let  $S^{in}$  and  $D$  be fixed. The graphs of the biogas flow rates functions

$$r \mapsto G_1(S^{in}, D, r), \text{ and } r \mapsto G_2(S^{in}, D, r),$$

445 are easily obtained from the graph of the output substrate concentration,  $r \mapsto$   
 446  $S_r^{out}(S^{in}, D)$ , see Fig. 4. Indeed, the formulas given in Proposition 4 show that,  
 447 whenever these functions are defined, we have

$$\begin{aligned} G_1(S^{in}, D, r) &= VD(S^{in} - S_r^{out}(S^{in}, D)), \\ G_2(S^{in}, D, r) &= VD(S^{in} - S_r^{out}(S^{in}, D)). \end{aligned}$$

448 We will see in Section 5, some illustrative plots of the biogas flow rates  $G_1$   
 449 and  $G_2$  as functions of the parameter  $r \in [0, 1]$ , for linear growth, see Fig. 7,  
 450 Monod growth, see Fig. 8 and Hill growth, see Fig. 9.

451 Let us illustrate the result of Proposition 5 by plotting the graphs of the  
 452 biogas flow rates

$$D \mapsto G_1(S^{in}, D, r) \text{ and } D \mapsto G_2(S^{in}, D, r),$$

453 when  $r$  and  $S^{in}$  are fixed, see Fig. 5. This figure is made without graduations on  
 454 the axes because it represents a general situation where the growth function is  
 455 only assumed to verify our hypotheses. Indeed the behaviors of the functions,  
 456 depicted in this figure, follow from our results and are not simply numerical  
 457 illustrations.

458 Notice that for any  $r \in (0, 1)$ , the graph of  $G_1$  (plotted in green in the  
 459 figure) is always below the graph  $G_{chem}$  (plotted in black). This illustrates  
 460 item 1 of Proposition 5. Assuming that Assumption 3 is satisfied, then for all  
 461  $0 < D < D_r(S^{in})$ , the graph of  $G_2$  (plotted in orange) is above the graph of  
 462  $G_{chem}$  (plotted in black). This illustrates item 2 of Proposition 5.

## 463 4.2 The maximal biogas of the serial configuration can 464 exceed that of the single chemostat

In Figure 5(c) the plot shows that the maximum of  $G_2$  (the red curve) is larger  
 than the maximum of  $G_{chem}$ , as we want to emphasize that the following  
 inequality is possible

$$\max_D G_2(S^{in}, D, r) > \max_D G_{chem}(S^{in}, D). \quad (41)$$

Indeed we will show that there is a value  $r^* \in (0, 1)$  such that this inequality is true for all  $r \in (r^*, 1)$ . The threshold  $r^*$  obviously depends on  $S^{in}$  and the rate of mortality  $a$ . It will be noted  $r^*(S^{in}, a)$  when we want to highlight this dependence. This phenomenon never occurs in the case of no mortality, since we have  $r^*(S^{in}, 0) = 1$ . Indeed, in the case without mortality, we proved, see Proposition 6 of [7], that for all  $S^{in} > 0$ , and all  $r \in (0, 1)$  we have

$$\max_D G_2(S^{in}, D, r) < \max_D G_{chem}(S^{in}, D),$$

465 that is to say, the maximal biogas flow rate of the serial configuration never  
466 exceed the maximal biogas flow rate of the single chemostat.

467 Let us prove that, when  $a > 0$ , the inequality (41) is always true for  $r$   
468 sufficiently close to 1. Observe that for any fixed  $S^{in} > \lambda(a)$  and  $r \in (0, 1]$ ,  
469 the continuous function  $D \mapsto G_2(S^{in}, D, r)$  is defined on the closed interval  
470  $[0, r(f(S^{in}) - a)]$ . It is null at the extremities of this interval and positive on  
471 the open interval  $(0, r(f(S^{in}) - a))$ . Therefore, it reaches its maximum. For a  
472 given  $S^{in} > \lambda(a)$ , we then consider the function

$$\overline{G}(r) := \max_{D \in [0, r(f(S^{in}) - a)]} G_2(S^{in}, D, r). \quad (42)$$

473 We want to ensure that this maximum is reached at a single value, denoted  
474  $\overline{D}(r)$ . Note that  $\overline{D}(1)$  represents the value, which we will assume to be unique,  
475 at which the function  $D \mapsto G_{chem}(S^{in}, D)$  reaches its maximum. We need the  
476 following assumption.

477 **Assumption 4** The function  $f$  is  $C^2$  and increasing and, for  $S^{in} > \lambda(a)$ , there  
478 exists  $\overline{D}(1) \in (0, f(S^{in}) - a)$  such that  $D \mapsto G_{chem}(S^{in}, D)$  is

- 479 • strictly concave at  $\overline{D}(1)$ ,
- 480 • increasing on  $(0, \overline{D}(1))$ ,
- 481 • decreasing on  $(\overline{D}(1), f(S^{in}) - a)$ ,

482 These conditions are related to the single chemostat model. They are ver-  
483 ified for linear, Monod, or Hill growth functions, see Remark 3 in Appendix  
484 A.

485 If Assumption 4 is satisfied, then the maximum of the function  $D \mapsto$   
486  $G_{chem}(S^{in}, D)$  is unique. The following lemma shows that the function  $D \mapsto$   
487  $G_2(S^{in}, D, r)$  satisfies the same property for  $r$  sufficiently close to 1.

488 **Lemma 4** Assume that Assumption 4 is satisfied, then for any  $S^{in} > \lambda(a)$ , there  
489 exists a neighborhood  $\mathcal{V}_1$  of 1, such that for any  $r \in \mathcal{V}_1 \cap \{r \leq 1\}$ , the maximum of  
490 the function  $D \mapsto G_2(S^{in}, D, r)$  is unique. We denote it by  $\overline{D}(r)$ . Moreover,  $\overline{D}$  is  
491 differentiable on  $\mathcal{V}_1 \cap \{r < 1\}$  with bounded derivative.

492 *Proof* The proof is given in in Appendix D.2. □

**Proposition 6** Under Assumption 4, the function  $\overline{G}$  admits left limits of its first and second derivatives at  $r = 1$ , which are

$$\overline{G}'(1^-) = 0, \quad \overline{G}''(1^-) = \frac{2a\overline{D}(1)}{\overline{D}(1) + a} (S^{in} - \lambda(\overline{D}(1) + a)). \quad (43)$$

493 *Proof* The proof is given in Appendix D.3. □

**Proposition 7** Under Assumption 4, there exists  $r^*$  in  $(0, 1)$  such that (41) is true for any  $r \in (r^*, 1)$  and

$$\max_D G_2(S^{in}, D, r^*) = \max_D G_{chem}(S^{in}, D).$$

*Proof* From Proposition 6, there exist  $\varepsilon > 0$  such that for all  $r \in (1 - \varepsilon, 1)$ , we have  $\overline{G}(r) > \overline{G}(1)$ . Therefore, the subset  $I$  of  $(0, 1)$  defined by

$$I = \{\rho \in (0, 1) : \forall r \in (\rho, 1), \overline{G}(r) > \overline{G}(1)\},$$

494 is non empty. Let  $r^*$  be the lower bound of  $I$ . We have  $\overline{G}(r^*) = \overline{G}(1)$  and  $\overline{G}(r) > \overline{G}(1)$   
 495 for  $r \in (r^*, 1)$ . Using (42), we deduce that the equality in the proposition is true and  
 496 (41) is true for any  $r \in (r^*, 1)$ . □

The function  $r \mapsto \overline{G}(r)$  reaches its maximum at some  $r^{max} \in (r^*, 1)$ . Let  $D^{max} = \overline{D}(r^{max})$  be the maximum of the function  $D \mapsto G_2(S^{in}, D, r^{max})$ . Therefore the maximal biogas flow rate of the serial chemostat is given by  $G_2(S^{in}, D^{max}, r^{max})$ . It satisfies

$$G_2(S^{in}, D^{max}, r^{max}) > G_{chem}(S^{in}, \overline{D}(1)).$$

497 We have plotted the function  $r \mapsto \overline{G}(r)$  for the linear, Monod, and Hill  
 498 growth functions considered in Fig. 6. It is seen in this figure that the tangent  
 499 at  $r = 1$  is horizontal which corresponds to  $\overline{G}'(1) = 0$ . In addition, one remarks  
 500 that  $\overline{G}(r) > \overline{G}(1)$  for  $r$  in some interval  $(r^*, 1)$  and  $\overline{G}(r^*) = \overline{G}(1)$ . Thus,  
 501 with presence of mortality rate, if practitioners are able to choose the dilution  
 502 rate  $D$ , the good strategy consists in working with a serial configuration and  
 503 choose  $r$  in the interval  $(r^*, 1)$ . The serial configuration should be operated at  
 504  $D = \overline{D}(r)$ , where  $\overline{D}(r)$  is defined in Lemma 4.

505 *Remark 2* • If one is interested in increasing the flow of biogas, the best choice  
 506 is  $r = r^{max}$ ,  $D = D^{max}$ .

507 • If one is interested in reducing the dilution rate, the best choice is  $r = r^*$   
 508 and  $D = D^*$ , where  $D^* = \overline{D}(r^*)$ .

Indeed, for the choice  $r = r^*$  and  $D = D^*$ , we have

$$G_2(S^{in}, D^*, r^*) = G_{chem}(S^{in}, \overline{D}(1)),$$

509 but  $D^*$  is expected to be significantly smaller than  $\overline{D}(1)$ , the dilution rate that  
510 maximises biogas for the simple chemostat. In fact, reducing  $D$  means that the  
511 flow rate  $Q$  has been reduced, and therefore energy has been saved to obtain  
512 the same result as with a simple chemostat

513 This result has an important message for practitioners: the serial config-  
514 uration is worth considering when mortality is not negligible. To the best of  
515 our knowledge, this result is new in the literature. On the other hand, it is not  
516 intuitive. For more information on this issue, see Section 5.4. For biological  
517 comments on the heuristic underlying this non-intuitive behaviour, the reader  
518 is referred to [6].

## 519 5 Illustrations and numerical simulations

520 This section illustrates of results using three different growth functions. As concave  
521 functions, we choose the linear growth function and the Monod function.  
522 As a non concave function, we choose the Hill function.

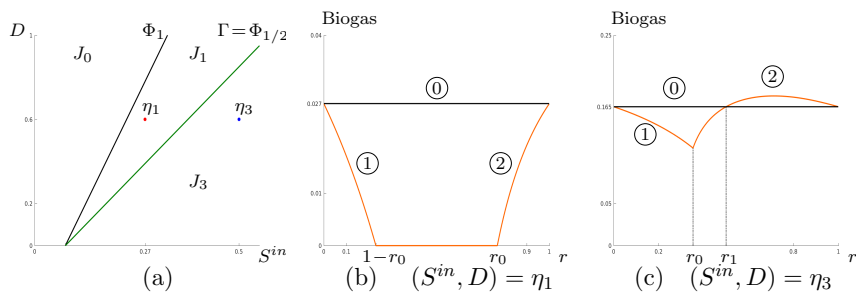


**Fig. 7** (a) The regions  $J_0$ ,  $J_1$  and  $J_3$  of the operating plane with  $f(S) = 4S$  and  $a = 0.3$ . The biogas flow rates corresponding to points  $\eta_1 = (0.27, 0.6) \in J_1$  and  $\eta_3 = (0.5, 0.6) \in J_3$  are depicted in panels (b) and (c) respectively. In these panels, the numbered curves ① (in black), and ② (in orange) are respectively defined by  $y = G_{chem}(S^{in}, D)$ ,  $y = G_1(S^{in}, D, r)$  and  $y = G_2(S^{in}, D, r)$ ;  $r_0(S^{in}, D) = D/(f(S^{in}) - a)$  and  $r_1(S^{in}, D)$  is defined by (20). (b)  $r_0 \approx 0.77$ . (c)  $r_0 \approx 0.35$  and  $r_1 = 0.5$ .

### 523 5.1 Linear growth function

524 Let consider a linear function  $f(S) = \alpha S$ ,  $\alpha > 0$ . As it is concave, according  
525 to item *ii* in Remark 1, the linear function verifies Assumptions 2 and 3.  
526 Therefore, our results apply for a linear function.

527 One has  $\lambda(2D + a) = g(D) = (2D + a)/\alpha$  then, the curves  $\Phi_{1/2}$ , defined by  
528 (13), and  $\Gamma$ , defined by (22), are identical. Consequently, the operating plane



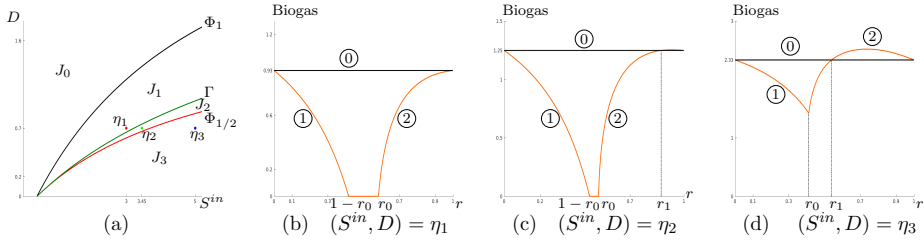


**Fig. 8** (a) The regions  $J_0$ ,  $J_1$ ,  $J_2$  and  $J_3$  in the operating plane with  $f(S) = 4S/(5+S)$  and  $a = 0.3$ . The biogas flow rates corresponding to points  $\eta_1 = (3, 0.7) \in J_1$ ,  $\eta_2 = (3.45, 0.7) \in J_2$  and  $\eta_3 = (5, 0.7) \in J_3$  are depicted in panels (b), (c) and (d) respectively. In these panels the curves are coloured and numbered as in Fig. 7,  $r_0(S^{in}, D) = D/(f(S^{in}) - a)$ , and  $r_1(S^{in}, D)$  is defined by (20) (b)  $r_0 \approx 0.58$ . (c)  $r_0 \approx 0.53$  and  $r_1 \approx 0.87$ . (d)  $r_0 \approx 0.41$  and  $r_1 \approx 0.54$ .

529  $(S^{in}, D)$  is divided in three regions  $J_i$ ,  $i = 0, 1, 3$  defined in (23) that describe  
 530 the behavior of the output substrate concentration and the biogas flow rate,  
 531 see Figure 7(a).

532 Consider the operating points  $\eta_1$  and  $\eta_3$ , fixed respectively in regions  $J_1$   
 533 and  $J_3$ , as shown in Figure 7(a). The behavior of the biogas flow rate for  
 534 these operating points is depicted in Figure 7(b,c). It should be noticed that  
 535 for any other point  $(S^{in}, D) \in J_1$ , the curve representing the biogas flow rate  
 536 with respect to  $r$  should be similar to the curve shown in Figure 7(a), and  
 537 corresponding to  $(S^{in}, D) = \eta_1$ . Similarly, for any other point  $(S^{in}, D) \in J_3$ ,  
 538 it should be similar to the curve shown in Figure 7(b), and corresponding to  
 539  $(S^{in}, D) = \eta_3$ .

540 In the linear case, the equation  $S^{in} = g_r(D)$  is a second degree algebraic  
 541 equation in  $r$  that gives two solutions, one corresponds to  $r_1(S^{in}, D)$  defined  
 542 by (20) and the other one is not considered as it does not belong to  $(0, 1)$ .

543 Since the point  $\eta_3 = (0.5, 0.6)$  satisfies the condition  $S^{in} > g(D)$ , as stated  
 544 in item 2 of Proposition 5, the serial configuration has a higher biogas flow  
 545 rate production than a single chemostat if and only if  $r \in (r_1, 1)$ , where  
 546  $r_1(0.5, 0.6) \approx 0.5$ , see Figure 7 (b).

## 547 5.2 Monod function

548 The Monod function is  $f(S) = mS/(K+S)$ . As it is concave, according to item  
 549 *ii* in Remark 1, the Monod function verifies Assumptions 2 and 3. Therefore,  
 550 our results apply for Monod function.

551 **Lemma 5** For any  $D > 0$ , the curve  $\Gamma$ , defined by (22), is at left of the curve  $\Phi_{1/2}$ ,  
 552 defined by (13).

553 *Proof* The curves  $\Phi_{1/2}$  and  $\Gamma$  are respectively defined by equations  $S^{in} = \lambda(2D + a)$   
 554 and  $S^{in} = g(D)$ . Let the function  $H : [0, (m - a)/2) \mapsto \mathbb{R}$  be defined by

$$H(D) = \lambda(2D + a) - g(D) = \frac{K_m D^2}{(m-D-a)^2(m-a-2D)}.$$

555 Note that  $H(0) = 0$  and, for any  $D \in (0, (m-a)/2)$ , one has  $H(D) > 0$  i.e.  $\lambda(2D +$   
 556  $a) > g(D)$ .

557 Hence, the curve  $\Gamma$  is at left of the curve  $\Phi_{1/2}$ . □

558 As a consequence of Lemma 5, the operating plane  $(S^{in}, D)$  is divided in  
 559 four regions  $J_i$ ,  $i = 0, 1, 2, 3$  defined in (23) that describe the behavior of the  
 560 output substrate concentration and the biogas flow rate, see Fig. 8(a).

561 Consider the operating points  $\eta_1, \eta_2$  and  $\eta_3$ , fixed respectively in regions  $J_1,$   
 562  $J_2$  and  $J_3$ , as shown in Fig. 8(a). The behavior of the biogas flow rate for these  
 563 points is depicted in Fig. 8(b,c,d). It should be noticed that for any other point  
 564  $(S^{in}, D) \in J_1$  (resp.  $(S^{in}, D) \in J_2$  and  $(S^{in}, D) \in J_3$ ), the curve representing  
 565 the biogas flow rate with respect to  $r$  should be similar to the curve shown  
 566 in Fig. 8(b) (resp. 8(c) and 8(d)), and corresponding to  $(S^{in}, D) = \eta_1$  (resp.  
 567  $(S^{in}, D) = \eta_2$  and  $(S^{in}, D) = \eta_3$ ).

568 In the Monod case, the equation  $S^{in} = g_r(D)$  is a second degree algebraic  
 569 equation in  $r$  that gives two solutions, one corresponds to  $r_1(S^{in}, D)$  defined  
 570 by (20) and the other one is not considered as it does not belong to  $(0, 1)$ .

571 Since the point  $\eta_2$  (resp.  $\eta_3$ ) satisfies the condition  $S^{in} > g(D)$ , as stated  
 572 in item 2 of Proposition 5, the serial configuration has a higher biogas flow  
 573 rate production than a single chemostat if and only if  $r \in (r_1, 1)$ , with  
 574  $r_1(3.45, 0.7) \approx 0.87$  in Fig.8(c) and  $r_1(5, 0.7) \approx 0.54$  in Fig. 8(c).

### 575 5.3 Hill function

576 The Hill function is  $f(S) = mS^p/(K^p + S^p)$ . Note that if  $p = 1$  this function  
 577 reduces to the Monod function. For  $p > 1$  it is non-concave. We have

$$\lambda(a) = \left(\frac{a}{m-a}\right)^{1/p} K.$$

578 **Proposition 8** *The Hill function satisfies the conditions (34) and (35). Therefore,*  
 579 *according to item iii in Remark 1, it verifies Assumption 2 and according to Lemma*  
 580 *3, it satisfies Assumption 3.*

581 *Proof* Let us first prove that the Hill function satisfies the condition (35). Straight-  
 582 forward computation give

$$\frac{d^2}{dS^2} \left( \frac{1}{f(S)-a} \right) = mpK^p \frac{(p+1)(m-a)S^{2p-2} + (p-1)aK^p S^{p-2}}{((m-a)S^p - aK^p)^3}.$$

583 Therefore,  $\frac{d^2}{dS^2} \left( \frac{1}{f(S)-a} \right) > 0$  for all  $S > \lambda(a)$ , that is to say, (35) is satisfied. This  
 584 result can also be obtained without laborious calculations by using item iii of Remark  
 585 1. Let  $\hat{S} \in (0, +\infty)$  be the inflexion point of the Hill function  $f$ . It is sufficient to  
 586 show that  $(1/f)'' > 0$  for all  $S \in (0, \hat{S})$ . One easily see that

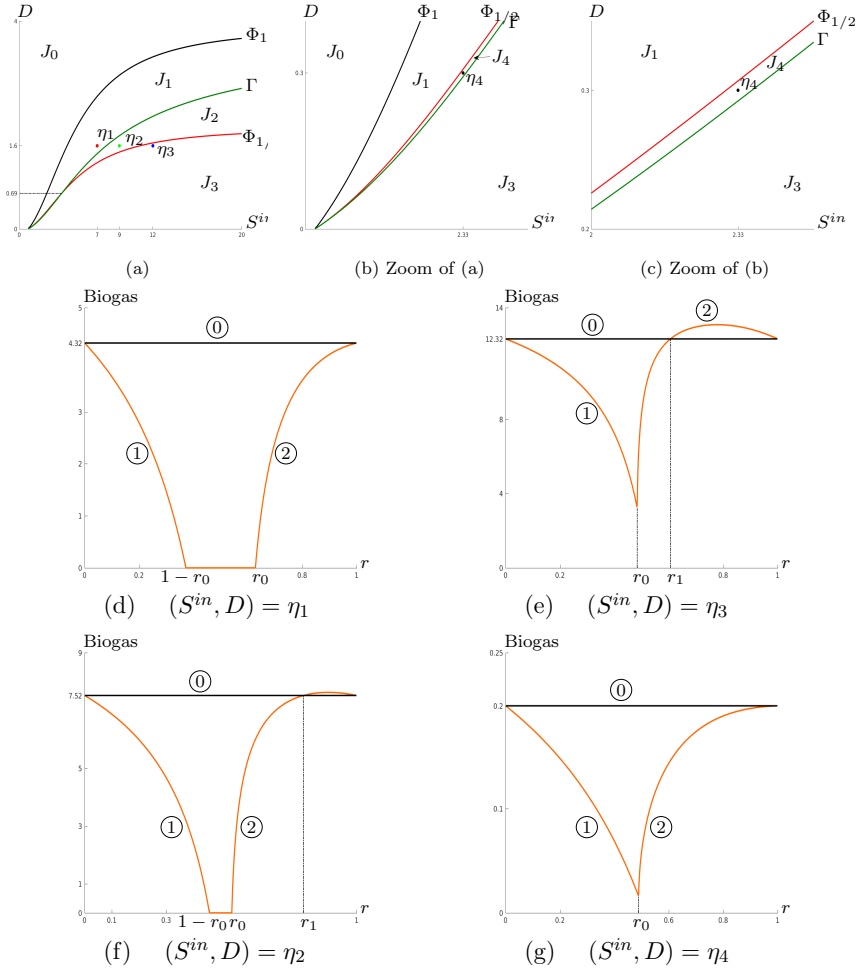


**Fig. 9** (a) The regions  $J_0, J_1, J_2, J_3$  and  $J_4$  in the operating plane with  $f(S) = 4S^2/(25 + S^2)$  and  $a = 0.1$ . The curves  $\Gamma$  and  $\Phi_{1/2}$  intersects for  $D_1 = 0.69$  (see Lemma 6). (b,c) Zooms of (a) showing the region  $J_4$ . The biogas flow rates corresponding to points  $\eta_1 = (7, 1.6) \in J_1$ ,  $\eta_2 = (9, 1.6) \in J_2$ ,  $\eta_3 = (12, 1.6) \in J_3$  and  $\eta_4 = (2.33, 0.3) \in J_4$  are depicted in panels (d) to (g), respectively. In these panels curves are coloured and numbered as in Fig. 7,  $r_0(S^{in}, D) = D/(f(S^{in}) - a)$ , and  $r_1(S^{in}, D)$  is defined by (20). (d)  $r_0 \approx 0.63$ . (e)  $r_0 \approx 0.54$  and  $r_1 \approx 0.81$ . (f)  $r_0 \approx 0.48$  and  $r_1 \approx 0.61$ . (g)  $r_0 \approx 0.49$ .

$$\left(\frac{1}{f}\right)''(S) = \frac{p(p+1)K^p}{mS^{p+2}} > 0,$$

587 for any  $S > 0$ . Consequently, for all  $p > 1$ , the Hill function verifies Assumption 2.

588 Let us now prove that the Hill function verifies the condition (34). Straightforward  
589 computations give

$$f'(\lambda(D + a)) = \frac{p}{K^m}(D + a)^{\frac{p-1}{p}}(m - a - D)^{\frac{p+1}{p}}. \quad (44)$$

590 Therefore,

$$f' \left( \lambda \left( \frac{D}{r} + a \right) \right) = \frac{p}{Km} \left( \frac{D}{r} + a \right)^{\frac{p-1}{p}} \left( m - a - \frac{D}{r} \right)^{\frac{p+1}{p}}.$$

591 Since  $p > 1$ ,  $D + ra < D + a$  and

$$0 < rm - ra - D < m - a - D,$$

592 one has

$$(D + ra)^{\frac{p-1}{p}} < (D + a)^{\frac{p-1}{p}} \quad (45)$$

$$(rm - ra - D)^{\frac{1}{p}} < (m - a - D)^{\frac{1}{p}}. \quad (46)$$

593 From (45) one has

$$\left( \frac{D}{r} + a \right)^{\frac{p-1}{p}} = \left( \frac{1}{r} \right)^{\frac{p-1}{p}} (D + ra)^{\frac{p-1}{p}} < \left( \frac{1}{r} \right)^{\frac{p-1}{p}} (D + a)^{\frac{p-1}{p}}. \quad (47)$$

594 On the other hand, we have

$$\left( m - a - \frac{D}{r} \right)^{\frac{p+1}{p}} = \left( \frac{1}{r} \right)^{\frac{1}{p}} \left( m - a - \frac{D}{r} \right) A,$$

595 where  $A = (rm - ra - D)^{\frac{1}{p}}$ . From (46), and using

$$0 < m - a - D/r < m - a - D,$$

596 we then deduce

$$\left( m - a - \frac{D}{r} \right)^{\frac{p+1}{p}} < \left( \frac{1}{r} \right)^{\frac{1}{p}} (m - a - D)^{\frac{p+1}{p}}. \quad (48)$$

597 Therefore, using (44), (47) and (48) one obtains

$$\begin{aligned} f' \left( \lambda \left( \frac{D}{r} + a \right) \right) &= \frac{p}{Km} \left( \frac{D}{r} + a \right)^{\frac{p-1}{p}} \left( m - a - \frac{D}{r} \right)^{\frac{p+1}{p}} \\ &< \frac{p}{Km} \frac{1}{r} (D + a)^{\frac{p-1}{p}} (m - a - D)^{\frac{p+1}{p}} = \frac{1}{r} f'(\lambda(D + a)). \end{aligned}$$

598 This ends the proof of (34). Consequently, according to Lemma 3, any Hill function  
599 satisfies Assumption 3.  $\square$

600 Let now consider the case  $p = 2$  of the Hill function:  $f(S) = mS^2/(K^2 + S^2)$ .

601 **Lemma 6** Let  $D_1 = (3m - 4a - \sqrt{m(5m - 4a)})/4$ . If  $0 < D < D_1$  then the curve  
602  $\Phi_{1/2}$ , defined by (13), at left of the curve  $\Gamma$ , defined by (22). In contrast, if  $D_1 < D < (m - a)/2$  then the curve  $\Phi_{1/2}$  is at right of the curve  $\Gamma$ .  
603

604 *Proof* Let the function  $H : [0, (m - a)/2) \mapsto \mathbb{R}$  be defined by  $H(D) := \lambda(2D + a) -$   
605  $g(D)$ . We have

$$H(D) = K \left( \sqrt{\frac{2D+a}{m-a-D}} - \frac{(2D+a)(m-a-D) + (D+a)(m-a)}{2(m-a-D)^{3/2} \sqrt{D+a}} \right).$$

606 Straightforward computation shows that this function is positive if and only if the  
607 polynomial

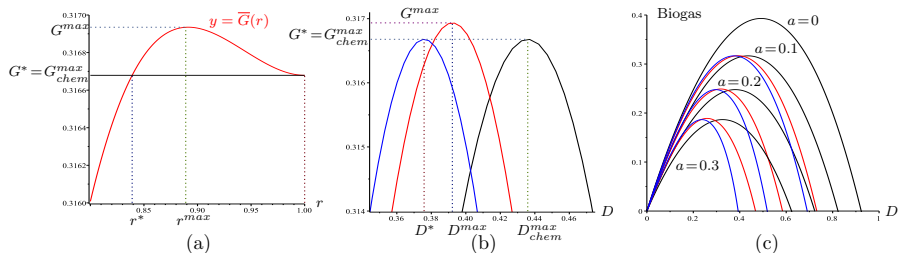


**Fig. 10** (a) The map  $r \mapsto \overline{G}(r)$  defined by (42), with  $f(S) = 4S/(5+S)$ ,  $a = 0.1$  and  $S^{in} = 1.5$ , showing the values  $r^*$  and  $r^{max}$ . (b) The corresponding maps  $D \mapsto G_{chem}(S^{in}, D)$ , in black,  $D \mapsto G_2(S^{in}, D, r^*)$ , in blue and  $D \mapsto G_2(S^{in}, D, r^{max})$ , in red, showing the values  $D^* < D^{max} < D_{chem}^{max}$ . (c) The biogas flow rates for  $a = 0, 0.1, 0.2, 0.3$  showing the effects of mortality.

$$Q(D) := 4D^2 - 2(3m - 4a)D + 4a^2 - 5am + m^2$$

608 is negative. The solution of equation  $Q(D) = 0$  are

$$D_1 = \frac{3m-4a-\sqrt{\Delta}}{4} \text{ and } D_2 = \frac{3m-4a+\sqrt{\Delta}}{4},$$

609 where  $\Delta = 4m(5m - 4a) > 0$ , as  $a < m$ . Notice that we have  $0 < D_1 < (m - a)/2$   
 610 and  $(m - a)/2 < D_2$ . Thus, for any  $D \in (D_1, (m - a)/2)$ , we have  $H(D) > 0$  and  
 611 then the curve  $\Phi_{1/2}$  at right of the curve  $\Gamma$ .  $\square$

612 As a consequence of Lemma 6, the operating plane is divided in five regions  
 613  $J_i$   $i = 0, 1, 2, 3, 4$  defined in (23), see Figure 9(a,b,c).

614 Consider the operating points  $\eta_1, \eta_2, \eta_3$  and  $\eta_4$  fixed respectively in regions  
 615  $J_1, J_2, J_3$  and  $J_4$ , as shown in Figure 9(a,b,c). It should be noticed that  
 616 for any other point  $(S^{in}, D) \in J_1$  (resp.  $(S^{in}, D) \in J_2, (S^{in}, D) \in J_3$  and  
 617  $(S^{in}, D) \in J_4$ ), the curve representing the biogas flow rate with respect to  
 618  $r$  should be similar to the curve shown in Fig. 9(a) (resp. (b), (c) and (d)),  
 619 and corresponding to  $(S^{in}, D) = \eta_1$  (resp.  $(S^{in}, D) = \eta_2, (S^{in}, D) = \eta_3$  and  
 620  $(S^{in}, D) = \eta_4$ ).

621 Recall that  $r_1(S^{in}, D)$  is defined by (20). It is obtained by solving numerically  
 622 the equation  $S^{in} = g_r(D)$ . Since the point  $\eta_2$  (resp.  $\eta_3$ ) satisfies the  
 623 condition  $S^{in} > g(D)$ , as stated in item 2 of Proposition 5, the serial configura-  
 624 tion has a higher biogas flow rate production than a single chemostat if and  
 625 only if  $r \in (r_1, 1)$ , with  $r_1(9, 1.6) \approx 0.81$  in Fig. 9(e) and  $r_1(12, 1.6) \approx 0.61$ , in  
 626 Fig. 9(f).

## 627 5.4 The serial configuration is worth considering when 628 mortality is not negligible

629 In this section we numerically illustrate Remark 2. We fix  $S^{in}$  and we adopt  
 630 the following notations.

$$D_{chem}^{max} = \overline{D}(1), \quad G_{chem}^{max} = \overline{G}(1) = G_{chem}(S^{in}, D_{chem}^{max})$$

631 where  $\overline{G}(r)$  is defined by (42) and  $\overline{D}(r)$  is as in Lemma 4. Recall that  $r^* \in (0, 1)$   
 632 satisfies

$$\overline{G}(r^*) = \overline{G}(1) = G_{chem}^{max}, \quad (49)$$

633 and  $\overline{G}(r) > \overline{G}(1)$  for  $r \in (r^*, 1)$ , so that  $\overline{G}(r)$  attains its maximum for  $r =$   
 634  $r^{max} \in (r^*, 1)$ , see Fig. 10(a), obtained with a Monod function and  $S^{in} = 1.5$ .  
 635 We adopt the following notations.

$$D^{max} = \overline{D}(r^{max}), \quad G^{max} = G_2(S^{in}, D^{max}, r^{max})$$

$$D^* = \overline{D}(r^*), \quad G^* = G_2(S^{in}, D^*, r^*) = G_{chem}^{max}$$

**Table 1** Numerical values

	$a = 0$	$a = 0.1$	$a = 0.2$	$a = 0.3$
$D_{chem}^{max}$	0.4918	0.4359	0.3806	0.3259
$G^* = G_{chem}^{max}$	0.3930	0.3167	0.2478	0.1866
$r^*$	1	0.839	0.717	0.631
$D^*$	0.4918	0.3758	0.2969	0.2369
$r^{max}$	1	0.889	0.808	0.751
$D^{max}$	0.4918	0.3925	0.3190	0.2591
$G^{max}$	0.3930	0.3169	0.2490	0.1890
$\frac{G^{max} - G_{chem}^{max}}{G_{chem}^{max}}$	0	0.06%	0.5%	1.3%
$\frac{D_{chem}^{max} - D^{max}}{D_{chem}^{max}}$	0	10%	16.2%	20.5%
$\frac{D_{chem}^{max} - D^*}{D_{chem}^{max}}$	0	13.6%	22%	27.3%

636 These notations are illustrated in Figs. 10(a,b). The zoom in Fig. 10(b)  
 637 shows that  $G^{max}$  exceeds  $G^* = G_{chem}^{max}$  only slightly, but  $D^*$  is significantly  
 638 smaller than  $D^{max}$ , which is itself smaller than  $D_{chem}^{max}$ . We give in Table 1 the  
 639 numerical values of  $r^*$ ,  $r^{max}$ ,  $D^*$ ,  $D^{max}$ ,  $G^{max}$  and  $G^* = G_{chem}^{max}$ , for various  
 640 values of the mortality rate  $a$ . The table also gives the relative gains

$$\frac{G^{max} - G_{chem}^{max}}{G_{chem}^{max}}, \quad \frac{D_{chem}^{max} - D^{max}}{D_{chem}^{max}}, \quad \frac{D_{chem}^{max} - D^*}{D_{chem}^{max}},$$

641 when replacing the single chemostat with the serial device using the ratios  $r^*$   
 642 and  $r^{max}$ . The gain in biogas production is almost negligible, but the gain in  
 643 bioreactor flow rate is significant.

644 The biogas flow rates  $G_{chem}(S^{in}, D)$ ,  $G_2(S^{in}, D, r^*)$  and  $G_2(S^{in}, D, r^{max})$ ,  
 645 for the various considered values of the mortality rate  $a$ , are depicted in Fig.  
 646 10(c), in black, blue and red, respectively. This figure shows that mortality is  
 647 a real problem as it considerably reduces biogas production. Where mortality  
 648 cannot be avoided or reduced, instead of using the single chemostat, by using  
 649 a serial device, biogas production can be slightly improved while significantly  
 650 reducing the bioreactor flow rate.

## 6 Conclusion

In this work, an in-depth study is carried out on the mathematical model of two interconnected chemostats in serial with mortality. Equations contain a term representing the mortality rate of the species. Due to this added term characterizing the mathematical model, this paper is considered as an extension of the work done in [7], where the model does not consider the mortality rate. However, the mathematical analysis revealed that the proofs have had to be significantly revisited and reveal several new non intuitive differences compared to the case without mortality. Let us recall that without mortality, the dynamics admits a forward attractive invariant hyperplane related to the total mass conservation, which is no longer verified under mortality consideration. This at the core of the differences in the mathematical analysis. The study of the model is based on the analysis of the asymptotic behavior of its solutions, and is supported by an operating diagram which describes the number and stability of steady states. In a first step, we considered different mortality rates  $a_1, a_2$  in each tank. Then, in view of comparing with the single configuration, we considered identical mortality rate  $a = a_1 = a_2$ . We analyzed the performances of the model at steady state for two different criteria: the output substrate concentration and the biogas flow rate (and compared them for the single chemostat with the same mortality rate  $a$ ). Explicit expressions of criteria, depending on the dilution rate  $D$  and the input substrate concentration  $S^{in}$ , are provided. These new results provide conditions that insure the existence of a serial configuration more efficient than a single chemostat, in the sense of minimizing the output substrate concentration or maximizing the biogas flow rate.

Along the paper, the similarities, specificities and differences of our model compared to the model without mortality (i.e. for  $a = 0$ ) studied in [7] are highlighted. Among the differences that attract attention, on the one hand, we have the operating diagram with different mortality which presents many more cases than the diagram without mortality where it is reduced to only two cases. Thus, the presence of the four regions of stability on the same diagram is now possible. On the other hand, we have the biogas production of the serial device in its maximum state which can be significantly larger than the largest biogas production of the single chemostat. This never happens in the case without mortality. Finally, unlike the case without mortality, the biomass productivity and the biogas flow rate at steady state are not given by the same formulas. Therefore, if biomass productivity is taken into account as a performance criterion, the comparison between the serial chemostat and the single chemostat does not lead to the same conclusions. For more details on this issue the reader can refer to [8].

## Appendix A The single chemostat

In this section, we give a brief presentation of the mathematical model of the single chemostat with mortality rate. The mathematical equations are given by

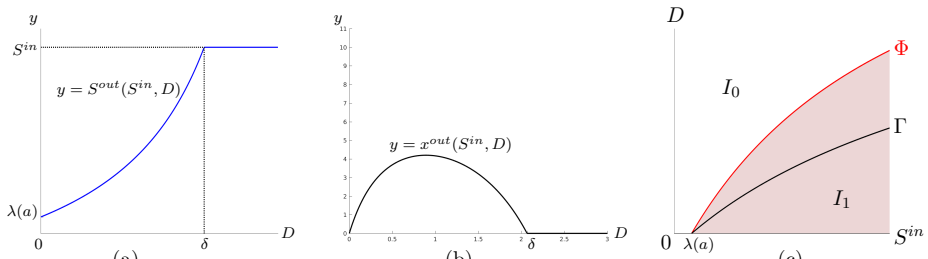


**Fig. A1** (a) The map  $D \mapsto S^{out}(S^{in}, D)$  is increasing on  $[0, \delta]$ , where  $\delta = f(S^{in}) - a$ . (b) The map  $D \mapsto x^{out}(S^{in}, D)$  with  $f(S) = 4S/(5 + S)$ ,  $S^{in} = 10$  and  $a = 0.6$ . (c) The curve  $\Gamma$  in the operating plane  $(S^{in}, D)$  of the single chemostat.

$$\begin{aligned} \dot{S} &= D(S^{in} - S) - f(S)x, \\ \dot{x} &= -Dx + f(S)x - ax, \end{aligned} \quad (\text{A1})$$

694 where  $S$  and  $x$  denote respectively the substrate and the biomass concentra-  
 695 tion,  $S^{in}$  the input substrate concentration,  $a$  the mortality rate and  $D = Q/V$   
 696 the dilution rate, with  $Q$  the input flow rate and  $V$  the volume of the tank.  
 697 The specific growth rate  $f$  of the microorganisms satisfies Assumption 1. It is  
 698 well known (see [16, 39]) that, besides the washout  $F_0 = (S^{in}, 0)$ , this system  
 699 can have a positive steady state

$$F_1 = (S^*(D), x^*(S^{in}, D)),$$

700 where

$$S^* = \lambda(D + a) \quad \text{and} \quad x^* = \frac{D}{D+a}(S^{in} - \lambda(D + a)).$$

701 See Fig. A1(a) for the plot of the function  $D \mapsto S^*(D)$  and Fig. A1(b) for the  
 702 plot of the function  $D \mapsto x^*(S^{in}, D)$  for  $0 \leq D \leq \delta$ , where  $\delta = f(S^{in}) - a$ .

703 The washout steady state  $F_0$  always exists. It is GAS if and only if  $D \geq \delta$ .  
 704 It is LES if and only if  $D > \delta$ . The positive steady state  $F_1$  exists if and only if  
 705  $D < \delta$ . It is GAS and LES whenever it exists. Therefore, the curve  $\Phi$  defined  
 706 by

$$\Phi := \{(S^{in}, D) : D = f(S^{in}) - a\} \quad (\text{A2})$$

707 splits the set of operating parameters  $(S^{in}, D)$  into two regions, denoted  $I_0$   
 708 and  $I_1$ , as depicted in A1(c). These regions are defined by

$$\begin{aligned} I_0 &:= \{(S^{in}, D) : D \geq f(S^{in}) - a\}, \\ I_1 &:= \{(S^{in}, D) : D < f(S^{in}) - a\}. \end{aligned} \quad (\text{A3})$$

709 The behavior of the system in each region is given in Table A1. Figure A1(c),  
 710 together with A1 is called the operating diagram of the single chemostat.

711 The particularity of this operating diagram is that the curve limiting both  
 712 regions  $I_0$  and  $I_1$  is translated from zero, unlike the case with mortality, as  
 713 shown in Figure 2.5 of [16]. Thus, with presence of mortality rate, the region  
 714 where the washout is GAS, is larger.



**Table A1** Stability of steady states in the various regions of the operating diagram.

	$I_0$	$I_1$
$F_0$	GAS	U
$F_1$		GAS

715 The output substrate concentration of the single chemostat, at its stable  
716 steady state is given by

$$S^{out}(S^{in}, D) = \begin{cases} S^{in} & \text{if } D \geq \delta \\ \lambda(D + a) & \text{if } D < \delta. \end{cases} \quad (\text{A4})$$

717 Its output biomass concentration at steady state is then given by

$$x^{out}(S^{in}, D) = \frac{D}{D+a}(S^{in} - S^{out}(D, a)) \quad (\text{A5})$$

718 For all  $S^{in} > \lambda(a)$ , one has

$$\frac{\partial S^{out}}{\partial D}(S^{in}, D) = \begin{cases} 0 & \text{if } D > \delta \\ \lambda'(D + a) & \text{if } D < \delta, \end{cases}$$

719 Thus, for any growth function satisfying Assumption 1 the function  $D \mapsto$   
720  $S^{out}(S^{in}, D)$  is increasing on  $[0, \delta]$ , as shown in Figure A1(a). The function  
721  $D \mapsto x^{out}(S^{in}, D)$  is illustrated in Figure A1(b) for a Monod function.

722 The biogas flow rate of the single chemostat is defined, up to a multiplica-  
723 tive yield coefficient, by

$$G_{chem}(S^{in}, D) := Vx^{out}f(S^{out}). \quad (\text{A6})$$

724 Using the expressions (A4) and (A5) respectively of  $S^{out}$  and  $x^{out}$ , the biogas  
725 flow rate of the single chemostat is given by:

$$G_{chem}(S^{in}, D) = \begin{cases} 0 & \text{if } D \geq \delta \\ VD(S^{in} - \lambda(D + a)) & \text{if } D < \delta. \end{cases} \quad (\text{A7})$$

726 For a given  $S^{in} > \lambda(a)$ , the function  $D \mapsto G_{chem}(S^{in}, D)$  is null for  $D = 0$  or  
727  $D \geq \delta$ , and is positive for  $D \in (0, \delta)$ . Therefore it admits a maximum in  $(0, \delta)$ ,  
728 which is assumed to be unique. A characterization of the growth functions for  
729 which this uniqueness is satisfied can be found in [31].

730 **Proposition 9** Assume that for any  $S^{in} > \lambda(a)$ , the maximum of  $D \mapsto$   
731  $G_{chem}(S^{in}, D)$  is unique, and define  $\bar{D}(S^{in}) \in (0, \delta)$ , such that

$$G_{chem}(S^{in}, \bar{D}(S^{in})) = \max_{D \geq 0} G_{chem}(S^{in}, D).$$

732 Then, the dilution rate  $D = \bar{D}(S^{in})$  is the solution of the equation  $S^{in} = g(D)$ ,  
733 where the function  $g : [0, m - a] \mapsto \mathbb{R}$  is given by

$$g(D) := \lambda(D + a) + D\lambda'(D + a). \quad (\text{A8})$$

735 *Proof* For any  $S^{in} > \lambda(a)$  and  $D \in (0, \delta)$ , we have

$$\frac{\partial G_{chem}}{\partial D}(S^{in}, D) = V \left( S^{in} - \lambda(D+a) - D\lambda'(D+a) \right) \quad (\text{A9})$$

736 Therefore,  $\frac{\partial G_{chem}}{\partial D}(S^{in}, D) = 0$  if and only if  $S^{in} = g(D)$ , where  $g$  is defined by  
737 (A8).  $\square$

738 Notice that the function  $g$  defined by (A8) is the same as the function  
739  $g$ , defined by (19), which was obtained as the limit, when  $r$  tends to 1, to  
740 the function  $g_r$ , defined by (9). Recall that  $\Gamma$  is the curve of equation  $S^{in} =$   
741  $g(D)$ , see (22). This curve is depicted in Fig. A1(c). It is the set of operating  
742 conditions given the higher biogas of the single chemostat. More precisely, for  
743 any  $S^{in} > \lambda(a)$ , the maximum  $D = \bar{D}(S^{in})$  of the biogas satisfies the condition  
744  $(S^{in}, D) \in \Gamma$ . Therefore, a sufficient condition for the uniqueness of  $\bar{D}(S^{in})$  is  
745 that the mapping  $g$  is increasing. If, in addition,  $f$  is  $\mathcal{C}^2$ , then, deriving (A9)  
746 with respect of  $D$ , we have

$$\frac{\partial^2 G_{chem}}{\partial D^2}(S^{in}, D) = -Vg'(D).$$

747 Hence, a sufficient condition for Assumption 4 to be satisfied is that  $g'(D) >$   
748  $0$  for  $D \in [0, m-a)$ . This last condition is satisfied whenever  $f'' \leq 0$  on  
749  $(\lambda(a), +\infty)$ , or  $\left(\frac{1}{f-a}\right)'' > 0$  on  $(\lambda(a), +\infty)$ , see Lemma 1 in [31]. Therefore we  
750 can make the following remark.

751 *Remark 3* Linear and Monod growth functions satisfy Assumption 4, since they  
752 satisfy  $f'' \leq 0$  on  $(0, +\infty)$ . On the other hand the Hill function satisfy Assumption  
753 4, since it satisfies  $\left(\frac{1}{f-a}\right)'' > 0$  on  $(\lambda(a), +\infty)$ , as shown in Proposition 8.

## 754 Appendix B The serial configuration

755 We consider a slight extension of system (1) with different mortality rates in  
756 the two tanks. Indeed, we assume that the growth environment differs from  
757 one tank to another one. This can lead to two different mortality rates in the  
758 tanks. We denote by  $a_1$  and  $a_2$  the mortality rates. The mathematical model  
759 is given by the following equations.

$$\begin{aligned} \dot{S}_1 &= \frac{D}{r}(S^{in} - S_1) - f(S_1)x_1 \\ \dot{x}_1 &= -\frac{D}{r}x_1 + f(S_1)x_1 - a_1x_1 \\ \dot{S}_2 &= \frac{D}{1-r}(S_1 - S_2) - f(S_2)x_2 \\ \dot{x}_2 &= \frac{D}{1-r}(x_1 - x_2) + f(S_2)x_2 - a_2x_2. \end{aligned} \quad (\text{B10})$$

760 The following result is classical in the mathematical theory of the chemo-  
761 stat.

762 **Lemma 7** For any nonnegative initial condition, the solution of system (B10)  
 763  $(S_1(t), x_1(t), S_2(t), x_2(t))$  is nonnegative for any  $t > 0$  and positively bounded.

764 *Proof* Since the vector field defined by (B10) is  $C^1$ , the uniqueness of the solution  
 765 to an initial value problem holds. From (B10) and using  $f(0) = 0$ , we have:

$$\begin{aligned} \text{for } i = 1, 2, \quad S_i = 0 &\implies \dot{S}_i > 0, \\ x_1 = 0 &\implies \dot{x}_1 = 0 \\ x_1 \geq 0 \text{ and } x_2 = 0 &\implies \dot{x}_2 \geq 0 \end{aligned}$$

766 Therefore, for  $i = 1, 2$ ,  $S_i(t) \geq 0$  and  $x_i(t) \geq 0$ , for all  $t \geq 0$ , for which they are  
 767 defined, provided  $S_i(0) \geq 0$  and  $x_i(0) \geq 0$ , for  $i = 1, 2$ , see Prop. B.7 in [39]. This  
 768 proves that the solutions of nonnegative initial conditions are always nonnegative.  
 769 Let  $z_i = S_i + x_i$ ,  $i = 1, 2$ . From system (B10), we have

$$z_1 = \frac{D}{r}(S^{in} - z_1) - a_1x_1, \quad z_2 = \frac{D}{1-r}(z_1 - z_2) - a_2x_2.$$

770 Consequently, we have the differential inequality

$$z_1 \leq \frac{D}{r}(S^{in} - z_1),$$

771 It follows by comparison of solutions of ordinary differential equations (see for  
 772 instance [48]) that one has

$$z_1(t) \leq S^{in} + (z_1(0) - S^{in})e^{-\frac{D}{r}t}$$

773 Therefore,  $z_1(t) \leq Z_1$ , where  $Z_1 = \max(S^{in}, z_1(0))$ . Then, we also have the  
 774 differential inequality

$$z_2 \leq \frac{D}{1-r}(Z_1 - z_2).$$

775 It follows again by comparison of solutions of ordinary differential equations that one  
 776 has also

$$z_2(t) \leq Z_1 + (z_2(0) - Z_1)e^{-\frac{D}{1-r}t}$$

777 Therefore,  $z_2(t) \leq Z_2$ , where  $Z_2 = \max(Z_1, z_2(0))$ . Hence, the solutions of (B10) are  
 778 positively bounded. Therefore, they are defined for all  $t \geq 0$ .  $\square$

779 For the description of the steady states, we shall consider the following  
 780 function  $h$  that will play a key role

$$\begin{aligned} h(S_2) &= \frac{D+(1-r)a_2}{1-r} \frac{S_1^* - S_2}{b - S_2}, \quad S_2 \in (0, b) \\ \text{where } S_1^* &= \lambda \left( \frac{D}{r} + a_1 \right), \quad b = \frac{D(S^{in} - S_1^*)}{D + ra_1} + S_1^*. \end{aligned} \tag{B11}$$

781 This function satisfies the following property.

782 **Lemma 8** Assume that  $D/r + a_1 < f(S^{in})$ . The function  $h$  is decreasing from  
 783  $h(0) > 0$  to  $h(S_1^*) = 0$ , where  $h(0)$  is given by

$$h(0) = \frac{D+(1-r)a_2}{1-r} \frac{(D+ra_1)S_1^*}{DS^{in} + ra_1S_1^*}. \tag{B12}$$

784 *Proof* From the condition  $D/r + a_1 < f(S^{in})$  it is deduced that  $S_1^* < S^{in}$ . Note that

$$b = \frac{DS^{in} + ra_1 S_1^*}{D + ra_1}.$$

785 Hence,  $b$  is a convex combination of  $S^{in}$  and  $S_1^*$ , and we have  $S_1^* < b < S^{in}$ .  
786 Therefore, the vertical asymptote  $S_2 = b$  of  $h$  is at right of  $S_1^*$ . The derivative of  $h$  is

$$h'(S_2) = \frac{D + (1-r)a_2}{1-r} \frac{S_1^* - b}{(b - S_2)^2}.$$

787 Hence, we have  $h'(S_2) < 0$  for all  $S_2 < b$ . Therefore,  $h$  is defined on the interval  
788  $(0, S_1^*)$  and is decreasing from  $h(0)$ , given by (B12) to  $h(S_1^*) = 0$ .  $\square$

789 Therefore, if  $D/r + a_1 < f(S^{in})$ , equation  $f(S_2) = h(S_2)$  admits a unique  
790 solution, denoted by  $S_2^*(S^{in}, D, r)$ , as shown in Fig. B2(a). This solution satisfy  
791 the following property.

792 **Lemma 9** *Considering  $a_1 = a_2 = a$ , for all  $0 \leq D < f(S^{in}) - a$ , one has*

$$\lim_{r \rightarrow 1} S_2^*(S^{in}, D, r) = \lambda(D + a).$$

793

794 *Proof* Let  $0 \leq D < f(S^{in}) - a$ . Using (5), the condition  $h(S_2) = f(S_2)$  is equivalent  
795 to

$$\begin{aligned} (D + (1-r)a)(S_1^* - S_2^*) &= \\ (1-r) \left( \frac{D}{D+ra}(S^{in} - S_1^*) + S_1^* - S_2^* \right) f(S_2^*). \end{aligned} \quad (\text{B13})$$

796 For  $r = 1$ , we have  $S_1^* = \lambda(D + a)$ . As  $\lim_{r \rightarrow 1} f(S_2^*) < +\infty$  then, (B13) gives

$$D(\lambda(D + a) - \lim_{r \rightarrow 1} S_2^*(S^{in}, D, r)) = 0.$$

797 Consequently, one has  $\lim_{r \rightarrow 1} S_2^*(S^{in}, D, r) = \lambda(D + a)$ .  $\square$

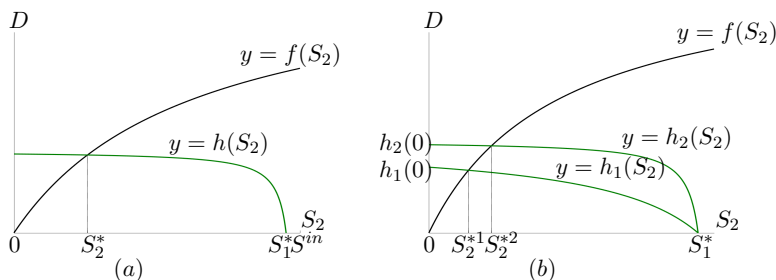


**Fig. B2** (a) Existence and uniqueness of the solution  $S_2^*$  of equation  $f(S_2) = h(S_2)$ . (b) Graphical illustration of Proposition 10:  $S_2^*$  decreases when  $S^{in}$  increases.

798 The existence and stability of steady states of (B10) are given by the  
799 following result.

800 **Theorem 3** Assume that Assumption 1 is satisfied. The steady states of (B10) are:

- The washout steady state  $E_0 = (S^{in}, 0, S^{in}, 0)$  which always exists. It is GAS if and only if

$$D \geq \max\{r(f(S^{in}) - a_1), (1-r)(f(S^{in}) - a_2)\}. \quad (\text{B14})$$

It is LES if and only if

$$D > \max\{r(f(S^{in}) - a_1), (1-r)(f(S^{in}) - a_2)\}.$$

- The steady state  $E_1 = (S^{in}, 0, \bar{S}_2, \bar{x}_2)$  of washout in the first chemostat but not in the second one with

$$\bar{S}_2 = \lambda \left( \frac{D}{1-r} + a_2 \right), \quad \bar{x}_2 = \frac{D}{D+(1-r)a_2} (S^{in} - \bar{S}_2). \quad (\text{B15})$$

It exists if and only if  $D < (1-r)(f(S^{in}) - a_2)$ . It is GAS if and only if

$$r(f(S^{in}) - a_1) \leq D \text{ and } D < (1-r)(f(S^{in}) - a_2). \quad (\text{B16})$$

It is LES if and only if

$$r(f(S^{in}) - a_1) < D < (1-r)(f(S^{in}) - a_2).$$

- The steady state  $E_2 = (S_1^*, x_1^*, S_2^*, x_2^*)$  of persistence of the species in both chemostats with

$$S_1^* = \lambda \left( \frac{D}{r} + a_1 \right), \quad x_1^* = \frac{D}{D+ra_1} (S^{in} - S_1^*), \quad (\text{B17})$$

$$x_2^* = \frac{D}{D+(1-r)a_2} \left( \frac{D}{D+ra_1} (S^{in} - S_1^*) + S_1^* - S_2^* \right) \quad (\text{B18})$$

801 and  $S_2^* = S_2^*(S^{in}, D, r)$  is the unique solution of the equation  $h(S_2) = f(S_2)$   
 802 with  $h$  defined by (B11). This steady state exists and is positive if and only  
 803 if  $D < r(f(S^{in}) - a_1)$ . It is GAS and LES whenever it exists and is positive.

804 *Proof* The 4-dimensional system of ODEs (B10) has a cascade structure of two planar  
 805 systems of ODEs, whose mathematical analysis is easy and well known in the  
 806 mathematical theory of the chemostat [16, 39]. Using this cascade structure, the  
 807 global behavior of the system is deduced from the global behaviour of planar systems  
 808 and Thieme's theory of asymptotically autonomous systems.

809 For the convenience of the reader the details of the proof are given in Appendix  
 810 D.1.  $\square$

811 **Proposition 10** The function  $S^{in} \mapsto S_2^*(S^{in}, D, r)$  is decreasing.

812 *Proof*  $D$  and  $r$  are fixed. Let  $S^{in,1} > S^{in,2}$  and  $h_i$  defined by (B11), with  $S^{in} = S^{in,i}$ ,  
 813  $i = 1, 2$ . Let  $S_2^{*i}$ , the solution of equation  $f(S_2) = h_i(S_2)$ ,  $i = 1, 2$ . Using Lemma  
 814 8,  $h_i$  is a decreasing hyperbola from  $h_i(0)$  defined by (B12), with  $S^{in} = S^{in,i}$ , to  
 815  $h_i(S_1^*) = 0$ . Since  $h_1(0) < h_2(0)$ , we have  $h_1(S_2) < h_2(S_2)$  for all  $S_2 \in (0, S_1^*)$ .  
 816 Therefore,  $S_2^{*1} < S_2^{*2}$ , see Fig. B2(b).  $\square$

817 This result means that the effluent steady state concentration of substrate  
 818 decreases when the influent concentration of substrate increases. This behavior  
 819 is very different from the single chemostat, where the effluent steady state  
 820 substrate concentration is independent of the influent substrate concentration.

## 821 Appendix C Operating diagram

822 For the chemostat model, the operating diagram has as coordinates the input  
 823 substrate concentration  $S^{in}$  and the dilution rate  $D$ , and shows how the solu-  
 824 tions of the system behave for different values of these two parameters. The  
 825 regions constituting the operating diagram correspond to different qualitative  
 826 asymptotic behaviors. Indeed, the main interest of an operating diagram is  
 827 to highlight the number and stability of the steady states for a given pair of  
 828 parameters  $(S^{in}, D)$ . The input substrate concentration  $S^{in}$  and the dilution  
 829 rate  $D$  are the usual parameters manipulated by the experimenter of a chemo-  
 830 stat. Apart from these parameters, and the parameter  $r$  that can be also chosen  
 831 by the experimenter but not easily changed as  $S^{in}$  and  $D$ , all other param-  
 832 eters have biological meaning and are fitted using experimental data from real  
 833 measurements of concentrations of micro-organisms and substrates. Therefore  
 834 the operating diagram is a bifurcation diagram, quite useful to understand the  
 835 possible behaviors of the solutions of the system from both the mathematical  
 836 and biological points of view.

837 Here, we fix  $r \in (0, 1)$  and we depict in the plane  $(S^{in}, D)$  the regions  
 838 in which the solution of system (B10) globally converges towards one of the  
 839 steady state  $E_0$ ,  $E_1$  or  $E_2$ . From the results given in Theorem 3, it is seen that  
 840 these regions are delimited by the curves  $\Phi_r^1$  and  $\Phi_{1-r}^2$  defined by:

$$\Phi_r^1 := \{(S^{in}, D) \in \mathbb{R}_+^2 : D = r(f(S^{in}) - a_1)\}, \quad (C19)$$

$$\Phi_{1-r}^2 := \{(S^{in}, D) \in \mathbb{R}_+^2 : D = (1-r)(f(S^{in}) - a_2)\}. \quad (C20)$$

841 When  $a_1 = a_2 = 0$ , as we have shown in [7], these curves meet only at one  
 842 point (the origin) and merge when  $r = 1/2$ . Therefore, in this case the curves  
 843  $\Phi_r^1$  and  $\Phi_{1-r}^2$  separate the operating plane  $(S^{in}, D)$ , in only three regions, see  
 844 [7, Figure 5]. This property continue to hold when  $a_1 = a_2$ , that is to say,  
 845 the curves intersect only at  $(\lambda(a_1), 0)$  and merge when  $r = 1/2$ . In this case  
 846 the curves  $\Phi_r^1$  and  $\Phi_{1-r}^2$  separate the operating plane  $(S^{in}, D)$ , in only three  
 847 regions, see Figure B3 (c) and (d). The novelty when  $a_1$  and  $a_2$  are different  
 848 and non null, is that the intersection of the curves  $\Phi_r^1$  and  $\Phi_{1-r}^2$  can lie outside  
 849 the  $S^{in}$  axis. Therefore there can be four regions in the operating plane, as  
 850 depicted in Figure B3 (a) and (f). For the description of the intersection of

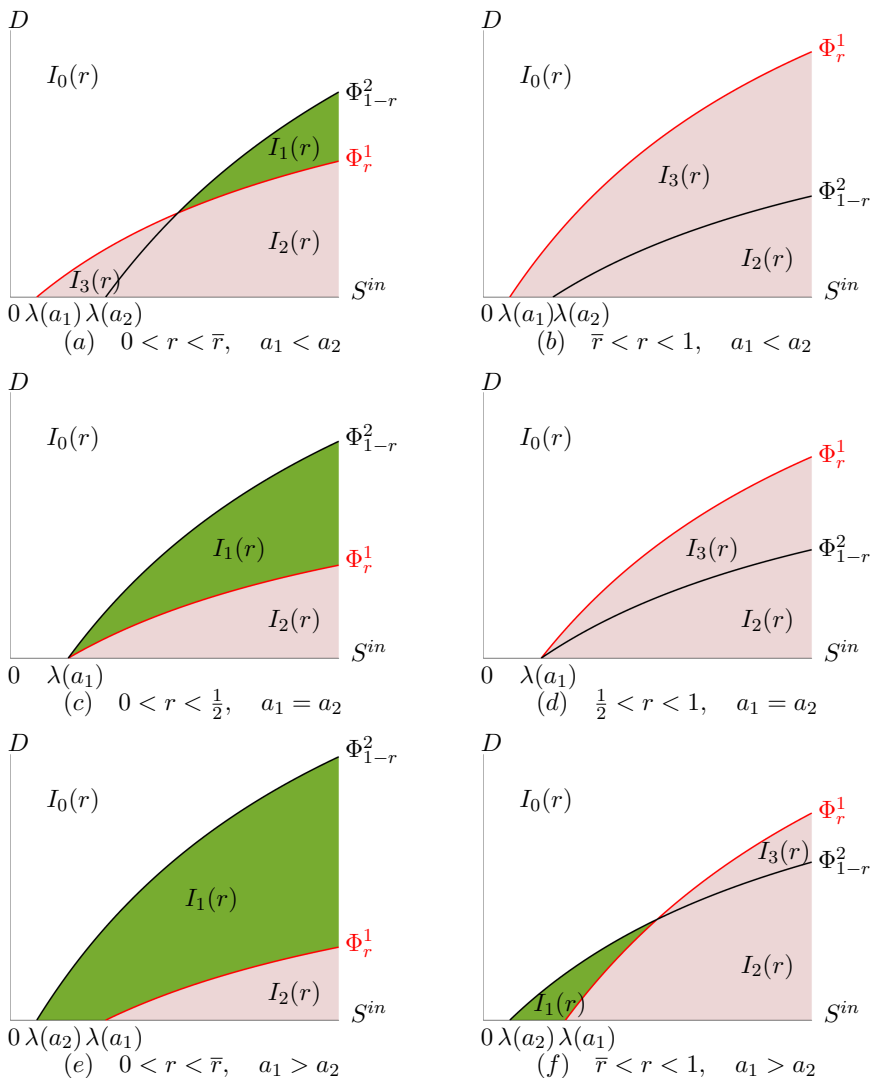


**Fig. B3** The operating diagram of (B10). The asymptotic behaviour in each region is depicted in Table C2.

851 the curves  $\Phi_r^1$  and  $\Phi_{1-r}^2$ , we need some definitions and notations. Let  $\bar{r} \in (0, 1)$   
 852 be defined by

$$\bar{r} := \frac{m-a_2}{2m-a_1-a_2}. \quad (\text{C21})$$

853 Note that if  $a_1 < a_2$  then  $\bar{r} < 1/2$ , and if  $a_1 > a_2$  then  $\bar{r} > 1/2$ . For  $a_1 < a_2$   
 854 and  $0 < r < \bar{r}$  (or  $a_1 > a_2$  and  $\bar{r} < r < 1$ ), we define the point  $P = (S_P^{\text{in}}, D_P)$   
 855 of the operating plane by:

**Table C2** The regions  $I_k(r)$ ,  $k = 0, 1, 2, 3$  of the operating diagram of (B10) and asymptotic behaviour in these various regions.

Regions
$I_0(r) = \{(S^{in}, D) : \max\{r(f(S^{in}) - a_1), (1-r)(f(S^{in}) - a_2)\} \leq D\}$
$I_1(r) = \{(S^{in}, D) : r(f(S^{in}) - a_1) \leq D \text{ and } D < (1-r)(f(S^{in}) - a_2)\}$ ,
$I_2(r) = \{(S^{in}, D) : 0 < D < \min\{r(f(S^{in}) - a_1), (1-r)(f(S^{in}) - a_2)\}\}$ ,
$I_3(r) = \{(S^{in}, D) : (1-r)(f(S^{in}) - a_2) \leq D \text{ and } D < r(f(S^{in}) - a_1)\}$ .

	$I_0(r)$	$I_1(r)$	$I_2(r)$	$I_3(r)$
$E_0$	GAS	U	U	U
$E_1$		GAS	U	
$E_2$			GAS	GAS

$$S_P^{in} := \lambda \left( \frac{ra_1 - (1-r)a_2}{2r-1} \right), \quad D_P := \frac{r(1-r)(a_2 - a_1)}{1-2r}. \quad (\text{C22})$$

856 Note that  $S_P^{in} > 0$  and  $D_P > 0$ . With these notations we can state the following  
857 result:

- 858 **Proposition 11** 1. If  $a_1 < a_2$  then for all  $r \in (0, \bar{r})$ , the curves  $\Phi_r^1$  and  $\Phi_{1-r}^2$   
859 intersect at the point  $P$  and  $\Phi_r^1$  is strictly below [resp. above]  $\Phi_{1-r}^2$  for  
860  $S^{in} > S_P^{in}$  [resp.  $S^{in} < S_P^{in}$ ], see Figure B3 (a). For all  $r \in (\bar{r}, 1)$ ,  $\Phi_r^1$  is  
861 strictly above  $\Phi_{1-r}^2$ , see Figure B3 (b).
- 862 2. If  $a_1 > a_2$  then for all  $r \in (\bar{r}, 1)$ , the curves  $\Phi_r^1$  and  $\Phi_{1-r}^2$  intersect at the  
863 point  $P$  and  $\Phi_r^1$  is strictly above [resp. below]  $\Phi_{1-r}^2$  for  $S^{in} > S_P^{in}$  [resp.  
864  $S^{in} < S_P^{in}$ ], see Figure B3 (f). For all  $r \in (0, \bar{r})$ ,  $\Phi_r^1$  is below  $\Phi_{1-r}^2$ , see  
865 Figure B3 (e).
- 866 3. If  $a_1 = a_2$  then, for  $r = 1/2$ ,  $\Phi_r^1 = \Phi_{1-r}^2$ . Moreover, if  $r < 1/2$  then  $\Phi_r^1$  is  
867 strictly below  $\Phi_{1-r}^2$ , see Figure B3 (c) and, if  $r > 1/2$  then  $\Phi_r^1$  is strictly  
868 above  $\Phi_{1-r}^2$ , see Figure B3 (d).

869 *Proof* For  $0 < r < 1$  and  $S^{in} > \lambda(a_i)$  we define the function  $\varphi_i$ ,  $i = 1, 2$ , by

$$\begin{aligned} \varphi_1(S^{in}, r) &= r(f(S^{in}) - a_1), \\ \varphi_2(S^{in}, r) &= (1-r)(f(S^{in}) - a_2). \end{aligned} \quad (\text{C23})$$

870 The curves  $\Phi_r^1$  and  $\Phi_{1-r}^2$ , defined respectively by (C19) and (C20), intersect if and  
871 only if there exists  $r \in (0, 1)$  and  $S^{in} > \max(\lambda(a_1), \lambda(a_2))$  such that  $\varphi_1(S^{in}, r) =$   
872  $\varphi_2(S^{in}, r)$ , that is to say

$$f(S^{in}) = A(r), \quad \text{with} \quad A(r) := \frac{ra_1 - (1-r)a_2}{2r-1}. \quad (\text{C24})$$

873 This equation has a solution  $S^{in} > \max(\lambda(a_1), \lambda(a_2))$  if and only if

$$\max(a_1, a_2) < A(r) < m, \quad (\text{C25})$$



874 where  $m = \sup(f)$ , as in (2). When these conditions are satisfied, the solution of  
 875 (C24) is given by  $S^{in} = \lambda(A(r))$ , where  $\lambda$  is the inverse function of  $f$ , i.e. the  
 876 break-even concentration defined by (3). Hence,  $S^{in} = S_P^{in}$ , given in (C22). The  
 877 corresponding intersection point of  $\Phi_r^1$  and  $\Phi_{1-r}^2$  is given by  $D_P = r(f(S_P^{in}) - a_1)$ ,  
 878 which is the value given in (C22).

879 Let us determine now for which value of  $r$ , the conditions (C25) are satisfied. The  
 880 function  $A$  is a homographic function. Its graphical representation is a hyperbola,  
 881 whose vertical asymptote is  $r = 1/2$ . Its derivative is given by

$$A'(r) = \frac{a_2 - a_1}{(2r - 1)^2}. \quad (\text{C26})$$

882 Note that  $A(r) = m$  if and only if  $r = \bar{r}$ , where  $\bar{r}$  is defined by (C21). Therefore  
 883 if  $a_1 < a_2$  then, according to (C26),  $A$  is increasing. Since  $A(0) = a_2$ ,  $A(\bar{r}) = m$ ,  
 884 and  $\bar{r} < 1/2$ , the condition (C25) is satisfied if and only if  $0 < r < \bar{r}$ . Similarly, if  
 885  $a_1 > a_2$ , then, according to (C26),  $A$  is decreasing. Since  $A(1) = a_1$ ,  $A(\bar{r}) = m$  and  
 886  $\bar{r} > 1/2$ , the condition (C25) is satisfied if and only if  $\bar{r} < r < 1$ . Finally, if  $a_1 = a_2$   
 887 then  $A(r) = a_1$  and the condition (C25) cannot be satisfied.

888 Suppose that  $a_1 < a_2$ . Note that for  $0 < r < 1/2$ , the condition  $f(S^{in}) > A(r)$   
 889 [resp.  $f(S^{in}) < A(r)$ ] is equivalent to  $\varphi_1(S^{in}, r) < \varphi_2(S^{in}, r)$  [resp.  $\varphi_1(S^{in}, r) >$   
 890  $\varphi_2(S^{in}, r)$ ]. Thus:

- 891 • If  $r \in (0, \bar{r})$ , then  $f(S^{in}) < A(r)$  if and only if  $S^{in} < S_P^{in}$ , where  $S_P^{in}$  is defined  
 892 by (C22). Hence, the curves  $\Phi_r^1$  and  $\Phi_{1-r}^2$  intersect at  $P = (S_P^{in}, D_P)$  and  
 893 the curve  $\Phi_r^1$  is strictly below [resp. above] the curve  $\Phi_{1-r}^2$ , for all  $S^{in} > S_P^{in}$   
 894 [resp.  $S^{in} < S_P^{in}$ ].
- 895 • If  $r \in [\bar{r}, 1/2)$  then  $f(S^{in}) < A(r)$  for all  $S^{in} > 0$ , so that the curve  $\Phi_r^1$  is  
 896 strictly above the curve  $\Phi_{1-r}^2$ .
- 897 • If  $r \in [1/2, 1)$ , then, using  $r \geq 1 - r$  and  $a_1 < a_2$ , one has  $\varphi_1(S^{in}, r) >$   
 898  $\varphi_2(S^{in}, r)$ . Therefore, the curve  $\Phi_r^1$  is strictly above the curve  $\Phi_{1-r}^2$ .

899 If  $a_1 > a_2$ , the proof is similar to the case  $a_1 < a_2$ .

900 If  $a_1 = a_2$  then  $\varphi_1(S^{in}, r) = \varphi_2(S^{in}, r)$  is equivalent to  $r(f(S^{in}) - a_1) = (1 -$   
 901  $r)(f(S^{in}) - a_1)$ . Therefore,  $r = 1 - r$ , that is  $r = 1/2$ . In this case the curves  $\Phi_r^1$  and  
 902  $\Phi_{1-r}^2$  merge. In addition, if  $r < 1/2$  [resp.  $r > 1/2$ ] then  $r < 1 - r$  [resp.  $r > 1 - r$ ]  
 903 and the curve  $\Phi_r^1$  is strictly below [resp. above] the curve  $\Phi_{1-r}^2$ . This ends the proof  
 904 of the proposition.  $\square$

905 For any  $r \in (0, 1)$ , the curves  $\Phi_r^1$  and  $\Phi_{1-r}^2$ , defined by (C19) and (C20),  
 906 respectively split the plane  $(S^{in}, D)$  in the regions denoted  $I_0(r)$ ,  $I_1(r)$ ,  $I_2(r)$   
 907 and  $I_3(r)$  and defined in Table C2. These regions are depicted in Fig. B3 in  
 908 the cases  $a_1 < a_2$ ,  $a_1 = a_2$  and  $a_1 > a_2$ .

909 The behavior of the system in each region, when it is not empty, is given in  
 910 Table C2. Notice that  $E_1$  exists in both regions  $I_1(r)$  and  $I_2(r)$ , but is stable  
 911 only when  $(S^{in}, D)$  is fixed in  $I_1(r)$ .

912 When  $a_1 = a_2 = 0$  then  $\lambda(a_1) = \lambda(a_2) = 0$  and the curves  $\Phi_r^1$  and  $\Phi_{1-r}^2$  of  
 913 the operating diagram start from the origin of the plane  $(S^{in}, D)$  and merge  
 914 for  $r = 1/2$ . Therefore, the diagrams shown in panels (a), (b), (c), (d), (e)  
 915 and (f) of Fig. B3 are reduced to only two different cases characterized by  
 916  $0 < r < 1/2$  and  $1/2 < r < 1$ , as shown in Figure 5 of [7]. There is no changes

917 in the stability of the steady states and in the number of the regions depicted  
918 in the operating diagram.

919 This result reveals an interplay between spatial heterogeneity (the ratio  $r$  of  
920 volume distribution between tanks) and the mortality heterogeneity (difference  
921 between  $a_1$  and  $a_2$ ). Indeed, panels (a) and (f) of Fig. B3 bring a particular  
922 feature when mortality rates are different: domains  $I_1(r)$  and  $I_3(r)$  can appear  
923 or disappear playing only with the spatial distribution  $r$ , a phenomenon which  
924 does not happens when mortality is identical in each tank. This shows that  
925 the existence of domains  $I_1(r)$  and  $I_3(r)$  is controlled by a relative toxicity in  
926 the tanks, and not only the spatial distribution as it is the case for identical  
927 mortality. This feature can have interest when practitioners can adjust  $pH$  or  
928 other abiotic parameters having impacts on the mortality rate, independently  
929 in each tank. Given operating parameters  $S^{in}$ ,  $D$  and  $r$ , panels (a) and (f) of  
930 Fig. B3 show that it is theoretically possible to pass from domain  $I_3(r)$  to  $I_2(r)$   
931 when mortality parameter is diminished only in the second tank. In practice,  
932 being in domain  $I_2(r)$  might be more desirable than  $I_3(r)$  with respect to some  
933 dysfunctioning of the first tank that can drop suddenly its biomass to zero.  
934 Indeed, in  $I_2(r)$ , the second tank is no conducted to the wash-out differently  
935 to the  $I_3(r)$  case.

936 When  $a_1 = a_2 = a$ , which is the case corresponding to the system (1)  
937 considered in Section 2, only panels (c,d) of Fig. B3 are encountered, as shown  
938 in Fig. 2. We describe hereafter the bifurcations that occur in this particular  
939 case. The general case i.e. when  $a_1 \neq a_2$  is similar.

940 *Remark 4* Transcritical bifurcations occur in the limit cases  $D = r(f(S^{in}) - a)$  and  
941  $D = (1 - r)(f(S^{in}) - a)$ , for system (1). If  $0 < r < 1/2$  then, we have a transcritical  
942 bifurcation of  $E_0$  and  $E_1$  when  $D = (1 - r)(f(S^{in}) - a)$  and a transcritical bifurcation  
943 of  $E_1$  and  $E_2$  when  $D = r(f(S^{in}) - a)$ . If  $1/2 < r < 1$  then, we have a transcritical  
944 bifurcation of  $E_0$  and  $E_1$  when  $D = (1 - r)(f(S^{in}) - a)$  and a transcritical bifurcation  
945 of  $E_0$  and  $E_2$  when  $D = r(f(S^{in}) - a)$ . If  $r = 1/2$  and  $D = (f(S^{in}) - a)/2$  then, we  
946 have transcritical bifurcations of  $E_0$  and  $E_1$ , and  $E_0$  and  $E_2$ , simultaneously.

## 947 Appendix D Proofs

### 948 D.1 Proof of Theorem 3

949 We begin by the existence of steady states. The steady states are the solutions  
950 of the set of equations  $\dot{S}_1 = 0$ ,  $\dot{x}_1 = 0$ ,  $\dot{S}_2 = 0$ ,  $\dot{x}_2 = 0$ . From equation  $\dot{x}_1 = 0$ ,  
951 it is deduced that  $x_1 = 0$  or  $f(S_1) = D/r + a_1$ . Suppose first that  $x_1 = 0$ .  
952 Then, from equation  $\dot{S}_1 = 0$  it is deduced that  $S_1 = S^{in}$  and from equation  
953  $\dot{x}_2 = 0$  it is deduced that  $x_2 = 0$  or  $f(S_2) = D/(1 - r) + a_2$ . If  $x_2 = 0$ ,  
954 then from equation  $\dot{S}_2 = 0$  it is deduced that  $S_2 = S^{in}$ . Hence we obtain the  
955 steady state  $E_0 = (S^{in}, 0, S^{in}, 0)$ , which always exist. On the other hand, if  
956  $f(S_2) = D/(1 - r) + a_2$ , then  $S_2 = \bar{S}_2$ , defined in (B15). From equation  $\dot{S}_2 = 0$ ,  
957 it is deduced that  $x_2 = \bar{x}_2$ , defined in (B15). Hence we obtain the steady state

958  $E_1 = (S^{in}, 0, \bar{S}_2, \bar{x}_2)$ . This steady state exists if and only if  $S^{in} > \bar{S}_2$ , that is  
 959  $D < (1-r)(f(S^{in}) - a_2)$ .

960 Suppose now that  $f(S_1) = D/r + a_1$ . Then  $S_1 = S_1^*$ , defined in (B17). From  
 961 equation  $\dot{S}_1 = 0$ , it is deduced that  $x_1 = x_1^*$ , defined in (B17). From equation  
 962  $\dot{S}_2 + \dot{x}_2 = 0$ , it is deduced that

$$x_2 = \frac{D}{D + (1-r)a_2}(S_1^* + x_1^* - S_2). \quad (\text{D27})$$

963 Replacing  $x_2$  by this expression in the equation  $\dot{S}_2 = 0$ , it is deduced that  
 964  $f(S_2) = h(S_2)$ , where  $h$  is defined by (B11). Hence  $S_2 = S_2^*$ , which is the  
 965 unique solution of the equation  $f(S_2) = h(S_2)$ , as shown in Figure B2 (a).  
 966 Replacing  $S_2$  by  $S_2^*$  in (D27) gives  $x_2 = x_2^*$ , defined by (B18). Consequently,  
 967 we obtain the steady state  $E_2 = (S_1^*, x_1^*, S_2^*, x_2^*)$ . This steady state is positive  
 968 if and only if  $S^{in} > S_1^*$ , which is equivalent to  $D < r(f(S^{in}) - a_1)$ .

969 Let us now study the local stability. Since the system has a cascade struc-  
 970 ture, the stability analysis reduces to the study of square  $2 \times 2$  matrices. Indeed,  
 971 the Jacobian matrix associated to system (B10) is the lower triangular matrix  
 972 by blocs,  $J = \begin{pmatrix} A & 0 \\ B & C \end{pmatrix}$  where  $B$  is the diagonal matrix whose diagonal elements  
 973 are  $D/(1-r)$ , and  $A$  and  $C$  are given by:

$$A = \begin{pmatrix} -\frac{D}{r} - f'(S_1)x_1 & -f(S_1) \\ f'(S_1)x_1 & -\frac{D}{r} + f(S_1) - a_1 \end{pmatrix},$$

$$C = \begin{pmatrix} -\frac{D}{1-r} - f'(S_2)x_2 & -f(S_2) \\ f'(S_2)x_2 & -\frac{D}{1-r} + f(S_2) - a_2 \end{pmatrix},$$

974 Hence, the eigenvalues of  $J$  are the ones of  $A$  and  $C$ .

975 For  $E_0$ , the eigenvalues are  $-D/r$ ,  $-D/r + f(S^{in}) - a_1$ ,  $-D/(1-r)$  and  
 976  $-D/(1-r) + f(S^{in}) - a_2$ . They are negative if and only if  $D > r(f(S^{in}) - a_1)$   
 977 and  $D > (1-r)(f(S^{in}) - a_2)$ . Therefore,  $E_0$  is LES if and only if the condition  
 978 in the theorem is satisfied.

979 For  $E_1$ , the eigenvalues of  $A$  are  $-D/r + f(S^{in}) - a_1$  and  $-D/r$ . The first  
 980 eigenvalue is negative if and only if  $D > r(f(S^{in}) - a_1)$ . On the other hand,  
 981 since the determinant of  $C$  is positive, and its trace is negative, the eigenvalues  
 982 of  $C$  are of negative real parts. Therefore,  $E_1$  is LES if and only if the condition  
 983 in the theorem is satisfied.

984 For  $E_2$ , the determinant of  $A$  is positive and its trace is negative. On the  
 985 other hand, using the notation  $C_{E_2}$  for the matrix  $C$  evaluated at  $E_2$ , we have

$$\det(C_{E_2}) = \left(-\frac{D}{1-r} - f'(S_2^*)x_2^*\right) \left(-\frac{D}{1-r} - a_2 + f(S_2^*)\right) + f(S_2^*)f'(S_2^*)x_2^*,$$

$$\text{tr}(C_{E_2}) = -2\frac{D}{1-r} - a_2 - f'(S_2^*)x_2^* + f(S_2^*).$$

986 Note that  $h(S_2) < D/(1-r) + a_2$  for all  $S_2 \in (0, S_1^*)$ . Therefore, from (B11),  
 987 we have  $f(S_2^*) = h(S_2^*) < D/(1-r) + a_2$ . Consequently,  $\det(C_{E_2})$  and  $\text{tr}(C_{E_2})$

988 are respectively positive and negative. Therefore,  $E_2$  is LES whenever it exists,  
989 that is  $D < r(f(S^{in}) - a_1)$ .

990 For the study of the global stability we use the cascade structure of the  
991 system (B10) and Thieme's Theorem (see Theorem A1.9 of [16]). In the rest of  
992 the proof, we denote by  $(S_1(t), x_1(t), S_2(t), x_2(t))$  the solution of (B10) with the  
993 initial condition  $(S_1^0, x_1^0, S_2^0, x_2^0)$ . Then,  $(S_1(t), x_1(t))$  is the solution of system

$$\begin{aligned}\dot{S}_1 &= \frac{D}{r}(S^{in} - S_1) - f(S_1)x_1 \\ \dot{x}_1 &= -\frac{D}{r}x_1 + f(S_1)x_1 - a_1x_1\end{aligned}\quad (\text{D28})$$

994 with initial condition  $(S_1^0, x_1^0)$  and  $(S_2(t), x_2(t))$  is the solution of the non-  
995 autonomous system of differential equations

$$\begin{aligned}\dot{S}_2 &= \frac{D}{1-r}(S_1(t) - S_2) - f(S_2)x_2 \\ \dot{x}_2 &= \frac{D}{1-r}(x_1(t) - x_2) + f(S_2)x_2 - a_2x_2\end{aligned}\quad (\text{D29})$$

996 with the initial condition  $(S_2^0, x_2^0)$ . The system (D28) is the classical model of  
997 a single chemostat. Its asymptotic behaviour is well known (see, for instance,  
998 Proposition 2.2 of [16]). This system admits the steady states:

$$e_0^1 = (S^{in}, 0) \quad \text{and} \quad e_1^1 = (S_1^*, x_1^*) \quad (\text{D30})$$

999 where  $S_1^*$  and  $x_1^*$  are defined by (B17). Two cases must be distinguished.

1000 Firstly, if  $\lambda(D/r + a_1) \geq S^{in}$ , that is  $D \geq r(f(S^{in}) - a_1)$  then,  $e_0^1$ , defined  
1001 in (D30), is GAS for (D28) in the nonnegative quadrant. Hence, for any non-  
1002 negative initial condition  $(S_1^0, x_1^0)$ ,

$$\lim_{t \rightarrow +\infty} (S_1(t), x_1(t)) = (S^{in}, 0). \quad (\text{D31})$$

1003 Therefore, the system (D29) is asymptotically autonomous with the limiting  
1004 system

$$\begin{aligned}\dot{S}_2 &= \frac{D}{1-r}(S^{in} - S_2) - f(S_2)x_2 \\ \dot{x}_2 &= -\frac{D}{1-r}x_2 + f(S_2)x_2 - a_2x_2.\end{aligned}\quad (\text{D32})$$

1005 Recall that the solutions of (D29) are positively bounded. Therefore, we shall  
1006 use Thieme's results which apply for bounded solutions.

1007 The system (D32) represents the classical model of a single chemostat. It  
1008 admits the two steady states  $e_0^2 = (S^{in}, 0)$  and  $e_1^2 = (\bar{S}_2, \bar{x}_2)$ , with  $(\bar{S}_2, \bar{x}_2)$   
1009 defined by (B15). Two subcases must be distinguished.

- 1010 • If  $\lambda(D/(1-r) + a_2) \geq S^{in}$ , that is  $D \geq (1-r)(f(S^{in}) - a_2)$  then,  
1011  $e_0^2$  is GAS in the nonnegative quadrant. Using Thieme's Theorem, we  
1012 deduce that for any nonnegative  $(S_2^0, x_2^0)$ , the solution  $(S_2(t), x_2(t))$  of  
1013 (D29) converges towards  $e_0^2 = (S^{in}, 0)$ . Using (D31) we deduce that,  
1014 when  $D \geq \max(r(f(S^{in}) - a_1), (1-r)(f(S^{in}) - a_2))$ , the solution  
1015  $(S_1(t), x_1(t), S_2(t), x_2(t))$  of (B10) converges towards  $E_0 = (S^{in}, 0, S^{in}, 0)$ ,  
1016 which proves (B14).

1017 • In contrast, if  $\lambda(D/(1-r) + a_2) < S^{in}$ , that is  $D < (1-r)(f(S^{in}) - a_2)$   
 1018 then, both steady states  $e_0^2$  and  $e_1^2$  exist and  $e_1^2$  is GAS in the positive quad-  
 1019 rant. Although system (D29) has the saddle point  $e_0^2$ , no polycycle can exist.  
 1020 Using Thieme's Theorem, for any positive  $(S_2^0, x_2^0)$ , the solution  $(S_2(t), x_2(t))$   
 1021 of (D29) converges towards  $e_1^2 = (\bar{S}_2, \bar{x}_2)$ . Using (D31) we deduce that,  
 1022 if  $r(f(S^{in}) - a_1) \leq D$  and  $D < (1-r)(f(S^{in}) - a_2)$ , then the solution  
 1023  $(S_1(t), x_1(t), S_2(t), x_2(t))$  of (B10) converges towards  $E_1 = (S^{in}, 0, \bar{S}_2, \bar{x}_2)$ ,  
 1024 which proves (B16).

1025 Secondly, if  $\lambda(D/r + a_1) < S^{in}$ , that is  $D < r(f(S^{in}) - a_1)$  then,  $e_1^1$ , defined  
 1026 in (D30), is GAS for (D28) in the positive quadrant. Hence, for any positive  
 1027 initial condition  $(S_1^0, x_1^0)$

$$\lim_{t \rightarrow +\infty} (S_1(t), x_1(t)) = (S_1^*, x_1^*). \quad (\text{D33})$$

1028 Therefore, the system (D29) is asymptotically autonomous with the limiting  
 1029 system

$$\begin{aligned} \dot{S}_2 &= \frac{D}{1-r}(S_1^* - S_2) - f(S_2)x_2 \\ \dot{x}_2 &= \frac{D}{1-r}(x_1^* - x_2) + f(S_2)x_2 - a_2x_2. \end{aligned} \quad (\text{D34})$$

1030 The system (D34) represents the classical model of a single chemostat with an  
 1031 input biomass. In this case, there is no washout and the system (D34) always  
 1032 admits one LES steady state  $e_2 = (S_2^*, x_2^*)$  with positive biomass defined by  
 1033 (B18) and  $S_2^*$  the unique solution of  $h(S_2) = f(S_2)$ .

1034 Let us show that this steady state is GAS for (D34). Assume that  $x_2 > 0$ .  
 1035 Consider the change of variable  $\xi = \ln(x_2)$ . The system (D34) becomes as

$$\begin{aligned} \dot{S}_2 &= \frac{D}{1-r}(S_1^* - S_2) - f(S_2)e^\xi \\ \dot{\xi} &= \frac{D}{1-r}(x_1^*e^{-\xi} - 1) + f(S_2) - a_2. \end{aligned} \quad (\text{D35})$$

The divergence of the vector field

$$\psi(S_2, \xi) = \begin{bmatrix} \frac{D}{1-r}(S_1^* - S_2) - f(S_2)e^\xi \\ \frac{D}{1-r}(x_1^*e^{-\xi} - 1) + f(S_2) - a_2 \end{bmatrix}$$

1036 associated to (D35) is  $\text{div} \psi(S_2, \xi) = -\frac{D}{1-r}(1 + x_1^*e^\xi) - f'(S_2)e^\xi$ . It is negative.  
 1037 Thus, using Bendixon-Dulac criterion, system (D35) cannot have a periodic  
 1038 solution. Hence, system (D34) has no cycle in the positive quadrant. For any  
 1039 non negative initial condition  $(S_2^0, x_2^0)$ , the solution of (D34) is bounded. Hence,  
 1040 the  $\omega$ -limit set of  $(S_2^0, x_2^0)$ , denoted  $\omega(S_2^0, x_2^0)$ , is non-empty and included in the  
 1041 positive quadrant. If  $e_2 \notin \omega(S_2^0, x_2^0)$  then, using Poincaré-Bendixon Theorem,  
 1042  $\omega(S_2^0, x_2^0)$  is a limit cycle, but the system does not present any, due to the  
 1043 divergence property. One then deduces  $e_2 \in \omega(S_2^0, x_2^0)$  and, as  $e_2$  is LES, then  
 1044  $\omega(S_2^0, x_2^0) = \{e_2\}$ . Consequently,  $e_2$  is GAS for (D34) in the positive quadrant.  
 1045 Using again Thieme's Theorem, for any positive  $(S_2^0, x_2^0)$ , the solution  
 1046  $(S_2(t), x_2(t))$  of (D29) converges towards  $e_2 = (S_2^*, x_2^*)$ . Using (D33) we deduce

1047 that, if  $D < r(f(S^{in}) - a_1)$ , then the solution  $(S_1(t), x_1(t), S_2(t), x_2(t))$  of (B10)  
 1048 converges towards  $E_2 = (S_1^*, x_1^*, S_2^*, x_2^*)$ . This ends the proof of the theorem.

## 1049 D.2 Proof of Lemma 4

1050 Let us fix  $S^{in}$  such that  $\delta := f(S^{in}) - a > 0$ . The proof consists in showing that  
 1051 the function  $(D, r) \mapsto G_2(S^{in}, D, r)$  can be formally extended as a  $C^2$  function  
 1052 for values of  $r$  larger than 1 (although such values have no physical meaning).  
 1053 Recall first that for any  $D \in (0, \delta)$ , one has  $G_2(S^{in}, D, 1) = G_{chem}(S^{in}, D)$ . As  
 1054  $G_2(S^{in}, \overline{D}(1), 1) > 0$  and  $G_2(S^{in}, 0, 1) = 0$ , there exists by continuity of the  
 1055 function  $G_2$ , numbers  $\underline{D} \in (0, \overline{D}(1))$ ,  $\underline{r} \in (0, 1)$  such that

$$G_2(S^{in}, D, r) < \max_{d \in (0, r\delta)} G_2(S^{in}, d, r), \quad (D, r) \in [0, \underline{D}] \times [\underline{r}, 1]. \quad (D36)$$

1056 Let  $\varepsilon > 0$  be such that

$$D_\varepsilon := \varepsilon \left( a + \max_{s \in [0, S^{in}]} f'(s)(S^{in} - s) \right) < \underline{D} \quad (D37)$$

1057 and consider the domain

$$\mathcal{D}_\varepsilon := \left\{ (D, r); \quad D \in (D_\varepsilon, \delta), \quad r \in \left( \max \left( \underline{r}, \frac{D}{\delta} \right), 1 + \varepsilon \right) \right\}.$$

1058 Note that for any  $(D, r) \in \mathcal{D}_\varepsilon$ , the number  $\lambda(D/r + a) = f^{-1}(D/r + a)$  is well  
 1059 defined. Posit the function

$$\begin{aligned} \varphi(S_2, D, r) &= (D + (1 - r)a) (\lambda(D/r + a) - S_2) \\ &\quad - (1 - r)f(S_2) \left( \frac{DS^{in} + ra\lambda(D/r + a)}{D + ra} - S_2 \right), \end{aligned}$$

1060 where  $(S_2, D, r) \in (0, S^{in}) \times \mathcal{D}_\varepsilon$ . As  $f$  is  $C^2$ ,  $\varphi$  is  $C^2$  on  $(0, S^{in}) \times \mathcal{D}_\varepsilon$ .

1061 For  $r < 1$  and  $(D, r) \in \mathcal{D}_\varepsilon$ , one has

$$\varphi(S_2, D, r) = (1 - r) \left( \frac{DS^{in} + ra\lambda(D/r + a)}{D + ra} - S_2 \right) (h(S_2) - f(S_2))$$

1062 where  $h$  is the function defined in (5). According to Lemma 8,  $h$  is posi-  
 1063 tive decreasing on  $(0, \lambda(D/r + a))$ , and  $h - f$  admits an unique zero  $S_2^* =$   
 1064  $S_2^*(S^{in}, D, r)$  on  $(0, \lambda(D/r + a))$ . Then, one can write

$$\partial_{S_2} \varphi \Big|_{S_2=S_2^*} = (1 - r) \left( \frac{DS^{in} + ra\lambda(D/r + a)}{D + ra} - S_2 \right) (\partial_{S_2} h - f') \Big|_{S_2=S_2^*} < 0.$$

1065 For  $r \in [1, 1 + \varepsilon)$  and  $(D, r) \in \mathcal{D}_\varepsilon$ , one has

$$\begin{aligned} \partial_{S_2} \varphi = & - (D + (1 - r)a) - (1 - r)f'(S_2) \left( \frac{DS^{in} + ra\lambda(D/r + a)}{D + ra} - S_2 \right) \\ & + (1 - r)f(S_2), \end{aligned}$$

1066 which is negative for any  $S_2 \in (0, S^{in})$  thanks to condition (D37). As  
 1067  $\varphi(0, D, r) > 0$  and  $\varphi(S^{in}, D, r) < 0$ , we deduce the existence of a unique  
 1068  $S_2^* = S_2^*(S^{in}, D, r)$  in  $(0, S^{in})$  such that  $\varphi(S_2^*, D, r) = 0$ , which also verifies  
 1069  $\partial_{S_2} \varphi < 0$  at  $S_2 = S_2^*$ .

1070 Then, by the Implicit Function Theorem, the function  $(D, r) \mapsto$   
 1071  $S_2^*(S^{in}, D, r)$  is  $C^2$  on  $\mathcal{D}_\varepsilon$ . Recall that for  $r < 1$  and  $D < r\delta$ , one has the  
 1072 expression  $G_2(S^{in}, D, r) = VD(S^{in} - S_2^*(S^{in}, D, r))$  (see Proposition 4). We  
 1073 extend now the function  $(D, r) \mapsto G_2(S^{in}, D, r)$  with this last  $C^2$  expression  
 1074 on  $\mathcal{D}_\varepsilon$ . As  $G_2(S^{in}, D, 1) = G_{chem}(S^{in}, D)$  for any  $D \in (0, \delta)$ , one deduces,  
 1075 by continuity of the partial derivatives of  $G_2$  with respect to  $D$  and property  
 1076 (D36), the existence of  $\mathcal{V}_D, \mathcal{V}_r$  as neighborhoods respectively of  $\bar{D}(1)$  and 1  
 1077 with  $\mathcal{V}_D \times \mathcal{V}_r \subset \mathcal{D}_\varepsilon$  such that for any  $r \in \mathcal{V}_r$ , the function  $D \mapsto G_2(S^{in}, D, r)$   
 1078 possesses the following properties

- 1079 1. it is strictly concave on  $\mathcal{V}_D$ ,
- 1080 2. it is increasing on  $(D_\varepsilon, \bar{D}(1)) \setminus \mathcal{V}_D$  and decreasing on  $(\bar{D}(1), r\delta) \setminus \mathcal{V}_D$ ,
- 1081 3. its maximum over  $(0, r\delta)$  is not reached for  $D \leq D_\varepsilon$ .

1082 We thus deduce that  $D \mapsto G_2(S^{in}, D, r)$  admits a unique maximum  $\bar{D}(r)$  on  
 1083  $(0, r\delta)$ , for any  $r \in \mathcal{V}_r$ .

1084 Finally, for any  $r \in \mathcal{V}_r$ ,  $\bar{D}(r)$  is characterized as the zero of the map  $D \mapsto$   
 1085  $F(D, r)$  where  $F$  is the  $C^1$  function

$$F(D, r) := \partial_D G_2(S^{in}, D, r)$$

1086 From property 1. above, one obtains

$$\partial_D F(\bar{D}(r), r) = \partial_{DD}^2 G_2(S^{in}, \bar{D}(r), r) < 0, \quad r \in \mathcal{V}_r$$

1087 and by the Implicit Function Theorem, there exists a neighborhood  $\mathcal{V}_1 \subset \mathcal{V}_r$   
 1088 of 1 such that  $\bar{D}$  is  $C^1$  on  $\mathcal{V}_1$ , which ends the proof of the lemma.

### 1089 D.3 Proof of Proposition 6

1090  $S^{in}$  being fixed, we shall drop the  $S^{in}$  dependency in the expressions of  $S_i^*, x_i^*$   
 1091 ( $i = 1, 2$ ) and  $G_2$ . Thus, let us define

$$\begin{aligned} G(D, r) &:= G_2(S^{in}, D, r), \\ F_i(D, r) &:= f(S_i^*(D, r))x_i^*(D, r), \quad i = 1, 2, \end{aligned}$$

1092 as functions of  $D \geq 0$  and  $r \in \mathcal{V}_1 \cap \{r < 1\}$ . Remark from the expression of  $F_1$ ,  
 1093 that it is well defined as well as its partial derivatives at  $r = 1$ . In addition,  
 1094 for the limiting case  $r = 1$ , using Lemma 9, for all  $D \geq 0$ , one has

$$\begin{aligned} S_2^*(D, 1) &= S_1^*(D, 1) = \lambda(D + a) \\ x_2^*(D, 1) &= x_1^*(D, 1) = \frac{D}{D+a}(S^{in} - \lambda(D + a)). \end{aligned} \quad (\text{D38})$$

1095 Thus, for all  $D \geq 0$ , one has

$$F_1(D, 1) = F_2(D, 1), \quad (\text{D39})$$

1096 and  $F_2$  is also well defined for  $r = 1$ . Thus, according to (37), for all  $D \geq 0$   
1097 and  $r \in \mathcal{V}_1 \cap \{r \leq 1\}$ , one has

$$G(D, r) = rF_1(D, r) + (1 - r)F_2(D, r),$$

1098 and from Lemma 4, for  $r \in \mathcal{V}_1 \cap \{r < 1\}$ , one has

$$\bar{G}(r) = G(\bar{D}(r), r), \quad (\text{D40})$$

1099 with  $\bar{G}$  defined by (42). For convenience, for a function  $E$  of  $(D, r)$  that is  
1100 differentiable, we shall define the three following functions:  $\bar{E}(r) := E(\bar{D}(r), r)$   
1101 and

$$\partial_r E(r) := \frac{\partial E}{\partial r}(\bar{D}(r), r), \quad \partial_D E(r) := \frac{\partial E}{\partial D}(\bar{D}(r), r).$$

1102 Therefore, the function  $\bar{G}$  writes

$$\bar{G}(r) = r\bar{F}_1(r) + (1 - r)\bar{F}_2(r), \text{ for } r \in \mathcal{V}_1 \cap \{r < 1\}. \quad (\text{D41})$$

1103 As the functions  $F_i$  are differentiable and as  $\bar{D}(r)$  is a maximizer of  $D \mapsto$   
1104  $rF_1(D, r) + (1 - r)F_2(D, r)$  on the interior of the interval  $[0, f(S^{in}) - a]$ , one has

$$r\partial_D F_1(r) + (1 - r)\partial_D F_2(r) = 0, \text{ for } r \in \mathcal{V}_1 \cap \{r < 1\}, \quad (\text{D42})$$

1105 and  $\partial_D F_1(1) = 0$ . As  $f$  is  $\mathcal{C}^2$  and  $\bar{D}$  is assumed to be differentiable on  $\mathcal{V}_1 \cap \{r <$   
1106  $1\}$ ,  $\bar{G}$  is differentiable and from (D41), for all  $r \in \mathcal{V}_1 \cap \{r < 1\}$ , one has

$$\begin{aligned} \bar{G}'(r) &= \bar{F}_1(r) - \bar{F}_2(r) + r\partial_r F_1(r) + (1 - r)\partial_r F_2(r) \\ &\quad + (r\partial_D F_1(r) + (1 - r)\partial_D F_2(r))\bar{D}'(r), \end{aligned}$$

1107 and with (D42), for all  $r \in \mathcal{V}_1 \cap \{r < 1\}$ , one has simply

$$\bar{G}'(r) = \bar{F}_1(r) - \bar{F}_2(r) + r\partial_r F_1(r) + (1 - r)\partial_r F_2(r). \quad (\text{D43})$$

1108 Let us now determine the limits of the terms of the right side of this last  
1109 equality when  $r$  tends to 1. Firstly, according to (D39), one has in particular

$$\bar{F}_1(1) = \bar{F}_2(1). \quad (\text{D44})$$

1110 Secondly, remark that the dynamics of the first tank is parameterized by  
1111 the single dilution rate  $D_1 = D/r$ , the other parameters being fixed (see the  
1112 expression (B17)). The function  $F_1$  takes then the form  $F_1(D, r) = \tilde{F}_1(D/r)$   
1113 where  $\tilde{F}_1$  is a smooth function. Therefore, one has

$$\partial_D F_1(r) = -\frac{r}{D(r)}\partial_r F_1(r). \quad (\text{D45})$$



1114 As  $\partial_D F_1(1) = 0$  then one deduces

$$\partial_r F_1(1) = 0. \quad (\text{D46})$$

1115 Finally, from  $\dot{S}_2 = 0$ , for all  $r \in \mathcal{V}_1 \cap \{r < 1\}$ , one gets

$$F_2(D, r) = \frac{D}{1-r} (S_1^*(D, r) - S_2^*(D, r)). \quad (\text{D47})$$

1116 Differentiating (D47) with respect to  $r$  gives

$$\frac{\partial F_2}{\partial r}(D, r) = \frac{D}{1-r} \left( \frac{\partial S_1^*}{\partial r}(D, r) - \frac{\partial S_2^*}{\partial r}(D, r) \right) + \frac{D}{(1-r)^2} (S_1^*(D, r) - S_2^*(D, r))$$

1117 which can be written equivalently as

$$(1-r) \frac{\partial F_2}{\partial r}(D, r) = D \left( \frac{\partial S_1^*}{\partial r}(D, r) - \frac{\partial S_2^*}{\partial r}(D, r) \right) + F_2(D, r).$$

1118 Thus, for  $D = \bar{D}(r)$ , one has

$$(1-r) \partial_r F_2(r) = \bar{D}(r) (\partial_r S_1^*(r) - \partial_r S_2^*(r)) + \bar{F}_2(r).$$

1119 Notice that for  $D = \bar{D}(r)$ , (D47) gives

$$\bar{F}_2(r) = \frac{\bar{D}(r)}{1-r} (\bar{S}_1^*(r) - \bar{S}_2^*(r)), \quad \text{for all } r \in \mathcal{V}_1 \cup \{r < 1\}. \quad (\text{D48})$$

1120 Using L'Hôpital's rule in (D48) when  $r$  tends to 1, one gets

$$\bar{F}_2(1) = \lim_{r \rightarrow 1^-} \frac{\bar{D}'(r)(\bar{S}_1^*(r) - \bar{S}_2^*(r)) + \bar{D}(r)(\partial_r S_1^*(r) - \partial_r S_2^*(r))}{-1}$$

1121 and using (D38) and (D44), one obtains

$$\bar{F}_1(1) = \lim_{r \rightarrow 1^-} -\bar{D}(r) (\partial_r S_1^*(r) - \partial_r S_2^*(r)).$$

1122 Consequently, one has

$$\lim_{r \rightarrow 1^-} (1-r) \partial_r F_2(r) = 0. \quad (\text{D49})$$

1123 With (D44), (D46) and (D49), expression (D43) gives the existence of the limit  
1124 of  $\bar{G}'$  when  $r$  tends to 1 with  $r < 1$ , which is

$$\bar{G}'(1^-) = 0. \quad (\text{D50})$$

1125 Note that  $\bar{G}''(1^-)$  exists if and only if  $\lim_{r \rightarrow 1^-} \frac{\bar{G}'(r) - \bar{G}'(1)}{r-1}$  exists. Using (D50)  
1126 and (D43), one has

$$\frac{\bar{G}'(r) - \bar{G}'(1^-)}{r-1} = -\frac{\bar{G}'(r)}{1-r} = -\frac{\bar{F}_1(r) - \bar{F}_2(r) + r \partial_r F_1(r) + (1-r) \partial_r F_2(r)}{1-r} \quad (\text{D51})$$

1127 On the one hand, using L'Hôpital's rule, one has

$$\lim_{r \rightarrow 1^-} \frac{\overline{F}_1(r) - \overline{F}_2(r)}{1 - r} = \lim_{r \rightarrow 1^-} \frac{\overline{F}'_1(r) - \overline{F}'_2(r)}{-1}.$$

1128 Recall that  $\partial_r F_1(1) = 0$  and thus one has  $\overline{F}'_1(1) = 0$ . Consequently, one has

$$\lim_{r \rightarrow 1^-} \frac{\overline{F}_1(r) - \overline{F}_2(r)}{1 - r} = \lim_{r \rightarrow 1^-} \overline{F}'_2(r) = \lim_{r \rightarrow 1^-} \partial_r F_2(r) + \partial_D F_2(r) \overline{D}'(r). \quad (\text{D52})$$

1129 On the other hand, using (D42) and (D45), one has

$$\frac{r}{1 - r} \partial_r F_1(r) = \frac{\overline{D}(r)}{r} \partial_D F_2(r). \quad (\text{D53})$$

1130 Thus, according to (D51), (D52) and (D53), one gets

$$\lim_{r \rightarrow 1^-} \frac{\overline{G}'(r) - \overline{G}'(1^-)}{r - 1} = \lim_{r \rightarrow 1^-} \quad (\text{D54})$$

1131 Let us show now that the limit of  $\partial_D F_2(r)$  is 0 when  $r$  tends to 1. One has

$$\frac{\partial F_2}{\partial D} = f'(S_2^*) \frac{\partial S_2^*}{\partial D} x_2^* + f(S_2^*) \frac{\partial x_2^*}{\partial D}.$$

1132 Let use the expression  $G(D, r) = D(S^{in} - S_2^*(D, r))$  given by Proposition 4.

1133 As  $\overline{D}(r)$  is a maximizer then one has

$$\partial_D G(r) = S^{in} - \overline{S}_2^*(r) - \overline{D}(r) \partial_D S_2^*(r) = 0.$$

1134 Using (D38), one then deduces

$$\partial_D S_2^*(1^-) = \frac{S^{in} - \lambda(\overline{D}(1) + a)}{\overline{D}(1)}.$$

1135 In addition, using expressions (B18) and (D38), one gets

$$\partial_D x_2^*(1^-) = -\frac{\overline{D}(1)}{(\overline{D}(1) + a)^2} (S^{in} - \lambda(\overline{D}(1) + a)),$$

1136 and hence the limit of  $\partial_D F_2$  when  $r$  tends to 1 exists:

$$\partial_D F_2(1^-) = \frac{S^{in} - \lambda(\overline{D}(1) + a)}{\overline{D}(1) + a} f'(\lambda(\overline{D}(1) + a)) A,$$

1137 where  $A = S^{in} - \lambda(\overline{D}(1) + a) - \frac{\overline{D}(1)}{f'(\lambda(\overline{D}(1) + a))}$ . Thus, one has

$$\partial_D F_2(1^-) = \frac{S^{in} - \lambda(\overline{D}(1) + a)}{\overline{D}(1) + a} f'(\lambda(\overline{D}(1) + a)) (S^{in} - g(\overline{D}(1))),$$

1138 with  $g$  defined by (A8). According to Proposition 9, one has  $S^{in} - g(\overline{D}(1)) = 0$ .

1139 Consequently, one has  $\partial_D F_2(1^-) = 0$ .

1140 Finally, it remains to calculate the limit of  $\partial_r F_2(r)$  when  $r$  tends to 1. One  
1141 has

$$\frac{\partial F_2}{\partial r} = f'(S_2^*) \frac{\partial S_2^*}{\partial r} x_2^* + f(S_2^*) \frac{\partial x_2^*}{\partial r}.$$

1142 Let us again use the expression  $G(D, r) = D(S^{in} - S_2^*(D, r))$ . According to (D41),  
1143 one has

$$\bar{G}'(r) = \partial_r G(r) + \partial_D G(r) \bar{D}'(r)$$

1144 where  $\partial_D G(r) = 0$ . According to (D50), we have  $\partial_r G(1^-) = 0$ , and thus  
1145  $\partial_r S_2^*(1^-) = 0$ . Using expression (B18), one gets

$$\partial_r x_2^*(1^-) = -a \bar{D}(1) \frac{S^{in} - \lambda(\bar{D}(1) + a)}{(\bar{D}(1) + a)^2},$$

1146 and then the limit of  $\partial_r F_2$  when  $r$  tends to 1 exists:

$$\partial_r F_2(1^-) = -a \bar{D}(1) \frac{S^{in} - \lambda(\bar{D}(1) + a)}{\bar{D}(1) + a}.$$

1147 As  $\bar{D}'$  is assumed to be bounded on  $\mathcal{V}_1 \cup \{r < 1\}$ , we thus obtain from  
1148 (D54) the existence of  $\bar{G}''(1^-)$  with

$$\bar{G}''(1^-) = -2\partial_r F_2(1^-)$$

1149 which is given by expression (43).

## 1150 Acknowledgements

1151 The authors thank Jérôme Harmand for valuable and fruitful comments.  
1152 The authors thank the Euro-Mediterranean research network Treasure (<http://www.inra.fr/treasure>).  
1153

## 1154 Conflict of interest

1155 The authors have no relevant financial or non-financial interests to disclose.

## 1156 Funding

1157 The authors declare that no funds, grants, or other support were received  
1158 during the preparation of this manuscript.

## 1159 Author Contributions

1160 All authors contributed to the study conception, methodology and mathe-  
1161 matical analysis. The first draft of the manuscript was written by Manel  
1162 Dali-Youcef. All authors commented on previous versions of the manuscript.  
1163 All authors read and approved the final manuscript.

## 1164 **Data Availability**

1165 Data sharing not applicable to this article as no datasets were generated or  
1166 analysed during the current study.

## 1167 **References**

- 1168 [1] N. Abdellatif, R. Fekih-Salem and T. Sari, Competition for a single  
1169 resource and coexistence of several species in the chemostat, *Math. Biosci.*  
1170 *Eng.*, 13 (2016), 631–652.
- 1171 [2] B. Bar and T. Sari, The operating diagram for a model of competition  
1172 in a chemostat with an external lethal inhibitor, *Discrete & Continuous*  
1173 *Dyn. Syst. - B*, 25 (2020), 2093–2120.
- 1174 [3] G. Bastin and D. Dochain, *On-line estimation and adaptive control of*  
1175 *bioreactors: Elsevier, Amsterdam, 1991.*
- 1176 [4] A. Bornhöft, R. Hanke-Rauschenbach and K. Sundmacher: steady state  
1177 analysis of the anaerobic digestion model no. 1 (adm1). *Nonlinear*  
1178 *Dynamics* 73 (2013), 535–549.
- 1179 [5] M. Crespo and A. Rapaport, About the chemostat model with a lateral  
1180 diffusive compartment, *Journal of Optimization, Theory and Applica-*  
1181 *tions*, Vol. 185 (2020), 597—621.
- 1182 [6] M. Dali-Youcef, J. Harmand, A. Rapaport, T. Sari. Some non-intuitive  
1183 properties of serial chemostats with and without mortality. 2021. <https://hal.archives-ouvertes.fr/03404740>
- 1184
- 1185 [7] M. Dali-Youcef, A. Rapaport and T. Sari, Study of performance criteria of  
1186 serial configuration of two chemostats, *Math. Biosci. Eng.*, 17(6) (2020),  
1187 6278-6309.
- 1188 [8] M. Dali-Youcef and T. Sari. The productivity of two serial chemostats  
1189 (2021). <https://hal.inrae.fr/hal-03445797>
- 1190 [9] Y. Daoud, N. Abdellatif, T. Sari and J. Harmand: Steady-state analysis  
1191 of a syntrophic model: The effect of a new input substrate concentration.  
1192 *Math. Model. Nat. Phenom.* 13 (2018), 31.
- 1193 [10] M. Dellal, M. Lakrib and T. Sari, The operating diagram of a model of  
1194 two competitors in a chemostat with an external inhibitor, *Math. Biosci.*,  
1195 302 (2018), 27–45.

- 1196 [11] R. Fekih-Salem, Y. Daoud, N. Abdellatif and T. Sari. A mathematical  
1197 model of anaerobic digestion with syntrophic relationship, substrate inhi-  
1198 bition and distinct removal rates. *SIAM Journal on Applied Dynamical*  
1199 *Systems* 20 (2021), 621–1654.
- 1200 [12] R. Fekih-Salem, C. Lobry and T. Sari, A density-dependent model of  
1201 competition for one resource in the chemostat, *Math. Biosci.*, 286 (2017),  
1202 104–122.
- 1203 [13] S. Fogler: *Elements of Chemical Reaction Engineering*, 4<sup>th</sup> edition.  
1204 Prentice Hall, New-York (2008).
- 1205 [14] C. de Gooijer, W. Bakker, H. Beeftink and J. Tramper, Bioreactors  
1206 in series: an overview of design procedures and practical applications.  
1207 *Enzyme Microb. Technol.* 18 (1996), 202–219.
- 1208 [15] I. Haidar, A. Rapaport, A. and F. Gérard, Effects of spatial structure and  
1209 diffusion on the performances of the chemostat. *Mathematical Bioscience*  
1210 and *Engineering.* 8(4) (2011), 953–971.
- 1211 [16] J. Harmand, C. Lobry, A. Rapaport and T. Sari, *The Chemostat: Mathe-*  
1212 *matical Theory of Microorganism Cultures*, John Wiley & Sons, Chemical  
1213 *Engineering Series*, 2017.
- 1214 [17] J. Harmand, A. Rapaport and A. Trofino, Optimal design of two  
1215 interconnected bioreactors—some new results. *AIChE J.* 49(6) (1999),  
1216 1433–1450.
- 1217 [18] Z. Khedim, B. Benyahia, B. Cherki, T. Sari and J. Harmand: Effect of  
1218 control parameters on biogas production during the anaerobic digestion  
1219 of protein-rich substrates. *Applied Mathematical Modelling* 61 (2018),  
1220 351–376.
- 1221 [19] C.M. Kung and B.C. Baltzis: The growth of pure and simple micro-  
1222 bial competitors in a moving and distributed medium. *Math. Biosci.* 111  
1223 (1992), 295–313 .
- 1224 [20] O. Levenspiel, *Chemical reaction engineering*, 3<sup>rd</sup> edition. Wiley, New York  
1225 (1999).
- 1226 [21] B. Li, Global asymptotic behavior of the chemostat : general response  
1227 functions and differential removal rates. *SIAM Journal on Applied*  
1228 *Mathematics* 59 (1998), 411–4.
- 1229 [22] R. W. Lovitt and J.W.T. Wimpenny, The gradostat: a tool for investi-  
1230 gating microbial growth and interactions in solute gradients. *Soc. Gen.*  
1231 *Microbial Quart.* 6 (1979), 80 .

- 1232 [23] R. W. Lovitt and J.W.T. Wimpenny, The gradostat: a bidirectional com-  
1233 pound chemostat and its applications in microbiological research, *J. Gen.*  
1234 *Microbiol.* 127 (1981), 261–268
- 1235 [24] K. Luyben and J. Tramper, Optimal design for continuously stirred tank  
1236 reactors in series using Michaelis-Menten kinetics. *Biotechnol. Bioeng.* 24  
1237 (1982), 1217–1220.
- 1238 [25] M. Nelson and H. Sidhu, Evaluating the performance of a cascade of two  
1239 bioreactors. *Chem. Eng. Sci.* 61 (2006), 3159–3166.
- 1240 [26] S. Pavlou, Computing operating diagrams of bioreactors, *J. Biotechnol.*,  
1241 71 (1999), 7–16.
- 1242 [27] M. Polihronakis, L. Petrou and A. Deligiannis, Parameter adaptive con-  
1243 trol techniques for anaerobic digesters—real-life experiments, Elsevier,  
1244 *Computers & chemical engineering*, 17(12) (1993), 1167-1179.
- 1245 [28] A. Rapaport, I. Haidar and J. Harmand, Global dynamics of the buffered  
1246 chemostat for a general class of growth functions, *J. Mathematical*  
1247 *Biology*, 71(1) (2015), 69–98.
- 1248 [29] A. Rapaport and J. Harmand, Biological control of the chemostat  
1249 with nonmonotonic response and different removal rates. *Mathematical*  
1250 *Biosciences and Engineering* 5, no. 3 (2008), 539–547.
- 1251 [30] T. Reh and J. Muller, CO<sub>2</sub> abatement costs of greenhouse gas (GHG)  
1252 mitigation by different biogas conversion pathways. *J. Environ. Manag.*  
1253 114, no. 15 (2013), 13–25.
- 1254 [31] T. Sari. Best Operating Conditions for Biogas Production in Some Simple  
1255 Anaerobic Digestion Models. *Processes* 2022, 10, 258.
- 1256 [32] T. Sari and B. Benyahia. The operating diagram for a two-step anaerobic  
1257 digestion model. *Nonlinear Dynamics* 2021, **105**, 2711–2737.
- 1258 [33] T. Sari and J. Harmand, A model of a syntrophic relationship between two  
1259 microbial species in a chemostat including maintenance, *Math. Biosci.*,  
1260 275 (2016), 1–9.
- 1261 [34] T. Sari and F. Mazenc, Global dynamics of the chemostat with different  
1262 removal rates and variable yields. *Math Biosci Eng.* 8(3) (2011), 827–40.
- 1263 [35] T. Sari and M.J. Wade, Generalised approach to modelling a three-tiered  
1264 microbial food-web, *Math. Biosci.*, 291 (2017), 21–37.
- 1265 [36] M. Sbarciog, M. Loccufer and E. Noldus, Determination of appropriate  
1266 operating strategies for anaerobic digestion systems, *Biochem. Eng. J.*, 51

1267 (2010), 180–188.

1268 [37] H. Smith, The gradostat: A model of competition along a nutrient  
1269 gradient. *Microbial Ecology*, 22(1) (1991), 207–26.

1270 [38] H. Smith, B. Tang and P. Waltman: Competition in a n-vessel gradostat.  
1271 *SIAM J. Appl. Math.* 91(5) (1991), 1451–1471.

1272 [39] H. Smith and P. Waltman, *The Theory of the Chemostat, Dynamics of*  
1273 *Microbial Competition*. Cambridge University Press, 1995.

1274 [40] B. Tang, Mathematical investigations of growth of microorganisms in the  
1275 gradostat, *J. Math. Biol.*, 23 (1986), 319–339.

1276 [41] M.J. Wade, R.W. Pattinson, N.G. Parker and J. Dolfing, Emergent  
1277 behaviour in a chlorophenol-mineralising three-tiered microbial ‘food  
1278 web’, *J. Theor. Biol.*, 389 (2016), 171–186.

1279 [42] M. Weederemann, G. Seo and G.S.K Wolkowics: Mathematical model of  
1280 anaerobic digestion in a chemostat: Effects of syntrophy and inhibition.  
1281 *Journal of Biological Dynamics* 7 (2013), 59–85.

1282 [43] M. Weederemann, G.S.K Wolkowicz and J. Sasara: Optimal biogas produc-  
1283 tion in a model for anaerobic digestion. *Nonlinear Dynamics* 81 (2015),  
1284 1097–1112.

1285 [44] G.S.K. Wolkowicz, Z. Lu, Global dynamics of a mathematical model of  
1286 competition in the chemostat: general response functions and differential  
1287 death rates. *SIAM Journal on Applied Mathematics* 52 (1992), 222–23.

1288 [45] A. Xu, J. Dolfing, T.P. Curtis, G. Montague and E. Martin, Maintenance  
1289 affects the stability of a two-tiered microbial ‘food chain’?, *J. Theor. Biol.*,  
1290 276 (2011), 35–41.

1291 [46] J. Zambrano and B. Carlsson, Optimizing zone volumes in bioreactors  
1292 described by Monod and Contois growth kinetics, *Proceeding of the IWA*  
1293 *World Water Congress & Exhibition*, (2014).

1294 [47] J. Zambrano, B. Carlsson and S. Diehl, Optimal steady-state design of  
1295 zone volumes of bioreactors with Monod growth kinetics. *Biochem. Eng.*  
1296 *J.* 100 (2015), 59–66.

1297 [48] W. Walter, *Ordinary Differential Equations*. Springer Graduate Texts in  
1298 *Mathematics*, 182 (1998).